NOAA Technical Report ERL 434–AOML 33 (Revised)

A Seasonal Isotherm Depth Climatology for the Eastern Tropical Pacific

Donald V. Hansen
Alan Herman

December 1988

U.S. DEPARTMENT OF COMMERCE
National Oceanic and Atmospheric Administration
Environmental Research Laboratories

NOAA Technical Report ERL 434–AOML 33 (Revised)

A Seasonal Isotherm Depth Climatology for the Eastern Tropical Pacific

Donald V. Hansen
Alan Herman

Atlantic Oceanographic and Meteorological Laboratory
Miami, Florida

December 1988

U.S. Department of Commerce
C. William Verity, Secretary

National Oceanic and Atmospheric Administration
William E. Evans, Under Secretary for Oceans and Atmosphere/Administrator

Environmental Research Laboratories
Boulder, Colorado
Vernon E. Derr, Director

NOTICE

Mention of a commercial company or product does not constitute an endorsement by NOAA Environmental Research Laboratories. Use for publicity or advertising purposes of information from this publication concerning proprietary products or the tests of such products is not authorized.

This report is published in revised form to correct a computer program error that was found subsequent to production of the original version by the same title, and to obtain better quality of reproductions of the maps than in the original.

For sale by the National Technical Information Service, 5285 Port Royal Road
Springfield, VA 22161

CONTENTS

A Seasonal Isotherm Depth Climatology for the Eastern Tropical Pacific

Donald V. Hansen and Alan Herman

ABSTRACT. A seasonal climatology of the depths of the 10°C, 15°C, and 20°C isotherms in the eastern tropical Pacific is presented. The analyses used Kriging, which is a method for optimal interpolation of data fields. The data set consisted of 10,505 expendable bathythermograph (XBT) and conductivity-temperature-depth (CTD) stations collected during non-El Niño years. Results are presented on shaded contour maps with values overprinted at 2° intervals. The method of analysis also yields an estimate of the uncertainty of each interpolated point.

1. INTRODUCTION

The Equatorial Pacific Ocean Climate Study (EPOCS) was begun by scientists of the National Oceanic and Atmospheric Administration (NOAA) in early 1979. The first years of this program consisted of exploratory studies and observations of the El Niño of 1982-1983. With the advent of the Tropical Oceans and Global Atmosphere (TOGA) program in 1985, EPOCS placed its emphasis on real-time observations and diagnosis of the evolution of El Niño/Southern Oscillation events in the tropical Pacific Ocean. These objectives, and experience during the 1982-1983 event, made clear that a climatological reference state was needed to put anomalous conditions into perspective. Consideration was given to use of the global atlas by Levitus (1982) for this purpose. However, because the Levitus atlas combines observations made during warm events with other observations, and a substantial number of new observations have been made subsequent to the observations available at that time, it was decided to undertake a modest new effort.

Because a principal objective of the effort is to facilitate delineation of the subsurface thermal pattern associated with El Niño, we decided to exclude observations made during El Niño events of record from the analyses. Our strategy also reduces to some extent the problems of bias due to extreme events in a modest data set, and to disproportionate numbers of observations being made during anomalous events (although some may prefer a climatology based on the full range of conditions experienced).

2. DATA SOURCES

The data base we used consists of 10,505 expendable bathythermograph (XBT) and conductivity-temperature-depth (CTD) casts. Data were from the years 1960, 1967, 1968, and 1980 through 1986 (excluding July 1982 through June 1983), from the following sources:

(1) Data from the Step-I expedition of 1960 (SIO, 1961).

(2) Data from the Eastern Tropical Pacific (EASTROPAC) international research project, consisting of seven 2-month survey periods during 1967 and 1968 (Love, 1971; Tsuchiya, 1974).

(3) CTD data from the cruises listed in Table 1.

(4) XBT data collected for the TOGA program by the NOAA Ships Discoverer, Oceanographer, and Researcher between 1984 and 1986.

(5) Scripps Institution of Oceanography ship-of-opportunity data for the year 1984.

(6) All XBT data, not duplicated above, made available through the Global Telecommunication System (GTS) from 1984 through 1986.

Preliminary analyses indicated that there were insufficient data to produce monthly mean climatological fields. Instead, the data were organized by season. The four seasons were defined as follows:

Winter:	December, January, February
Spring:	March, April, May
Summer:	June, July, August
Fall:	September, October, November.

Data locations are shown on Figs. 1-4.

Table 1.--Ships and cruise dates for recent CTD data collection

Ship	Organization	Cruise dates
Discoverer	NOAA	19 Feb.-18 Mar. 1982 24 Mar.-27 Apr. 1982 7 May -22 May 1982
Endeavor	Oregon State University	Nov. 1983 Apr. 1984 May 1984
Oceanographer	NOAA	6 Feb.- 6 Mar. 1980 21 Mar.-19 Apr. 1980 23 Feb.-24 Mar. 1981 25 May -23 June 1981 27 June-29 July 1981
Researcher	NOAA	28 July-21 Aug. 1980 26 Aug.-19 Sep. 1980 14 Oct.-14 Nov. 1981 21 Nov.- 7 Dec. 1981 17 July-24 Aug. 1983 9 Apr.- 8 May 1984 May -June 1984 9 Oct.- 5 Nov. 1984 13 Nov.-13 Dec. 1984 22 Sep.-18 Oct. 1985 29 Oct.-26 Nov. 1985 Nov.-Dec. 1985

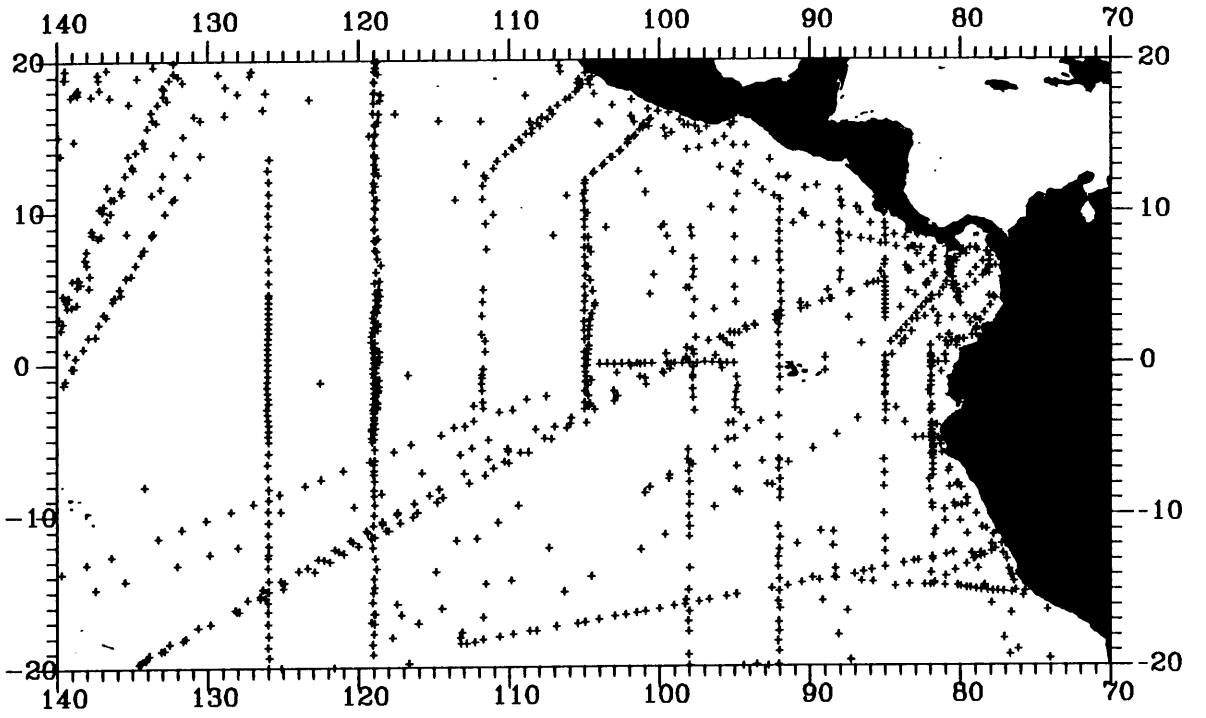

Figure 1.—Locations of stations used for the winter-season climatology (December-February), in the region 20°N-20°S and 70°W-140°W.

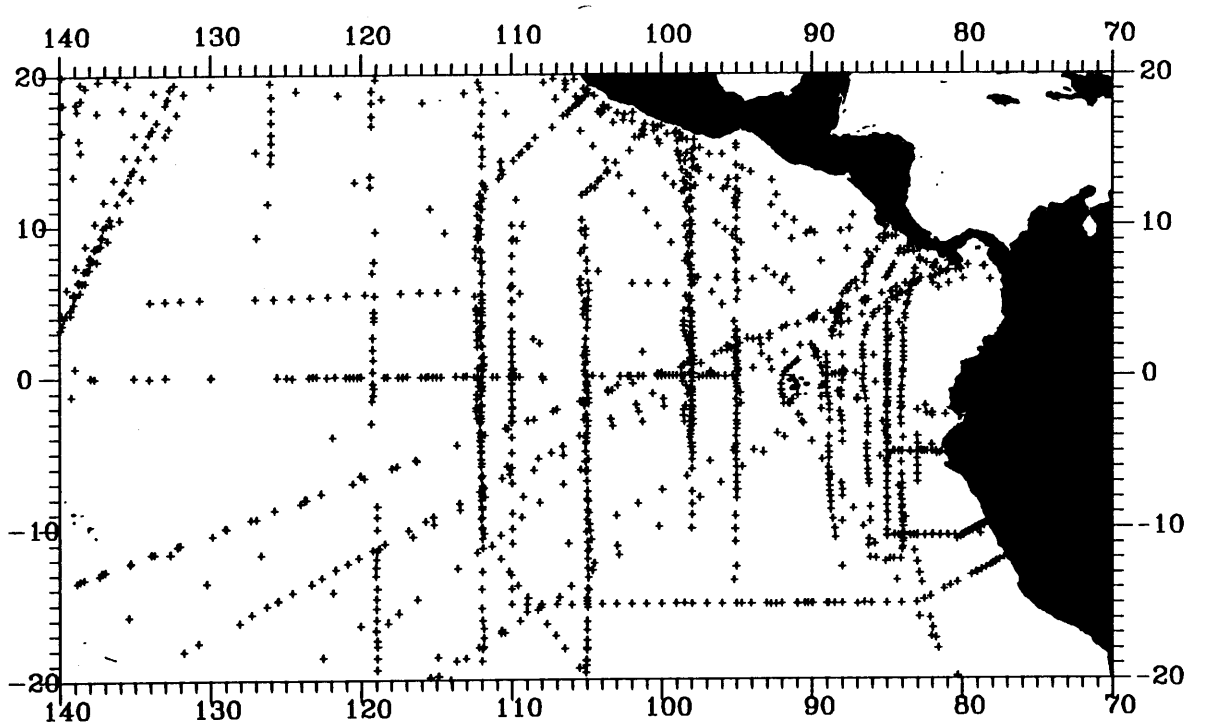

Figure 2.—Locations of stations used for the spring-season climatology (March-May), in the region 20°N-20°S and 70°W-140°W.

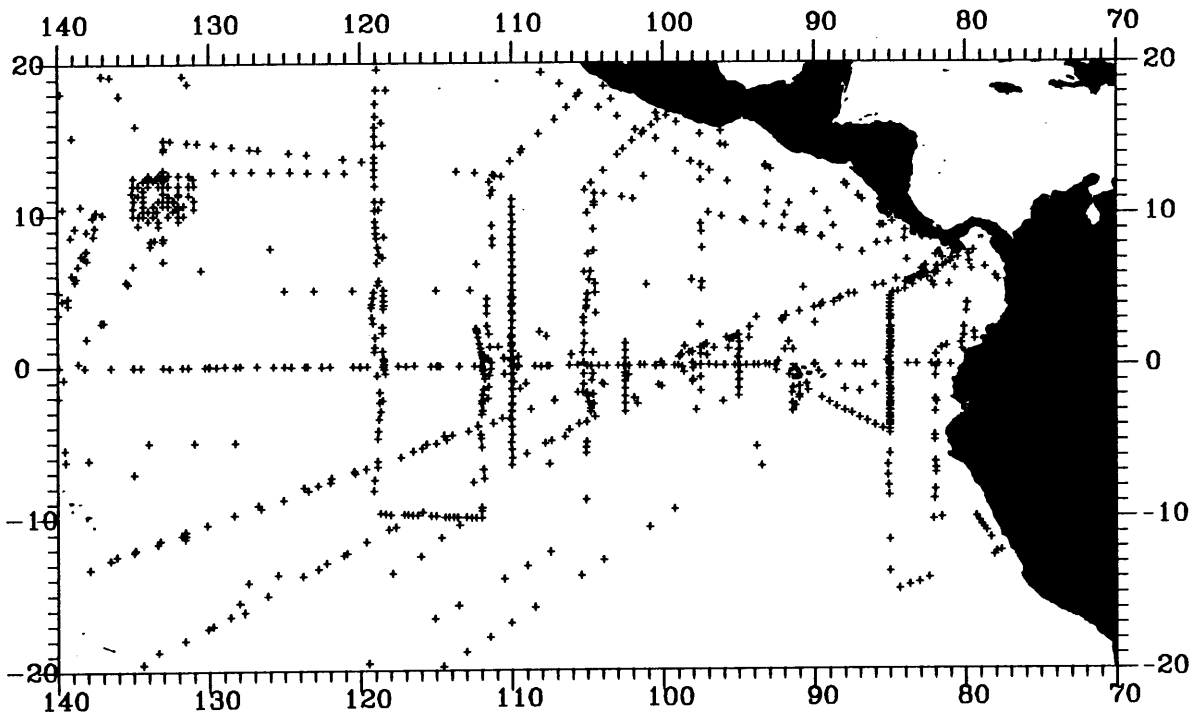

Figure 3.--Locations of stations used for the summer-season climatology (June-August), in the region 20°N-20°S and 70°W-140°W.

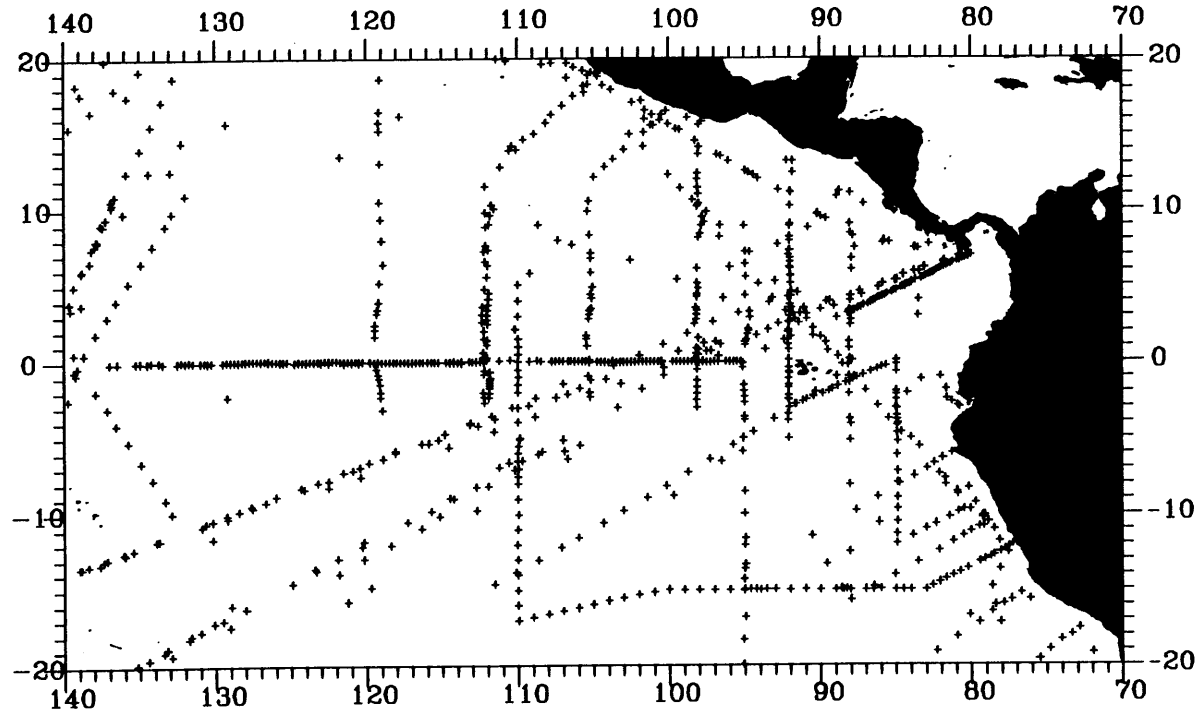

Figure 4.--Locations of stations used for the fall-season climatology (September-November), in the region 20°N-20°S and 70°W-140°W.

3. METHOD OF ANALYSES

Most of the data used were from carefully quality-controlled data sets collected for the EASTROPAC, EPOCS, First GARP Global Experiment (FGGE), and TOGA programs, so only checks for gross errors in transcription were required. The XBT data disseminated via the GTS, however, typically contain several kinds of errors. Erroneous data were deleted from the data set by identifying "bullseyes" in the data fields for each level.

The data were interpolated to a uniform 2° latitude by 2° longitude array for computer contouring by means of a method for optimum interpolation (OI) known as Kriging, after D. G. Krige, a pioneer in the field of geostatistics. The method is described briefly by Gandin (1963) and has been developed and used extensively in mining engineering and other terrestrial applications. An elementary discussion of the method is given by Clark (1979), and an extensive treatment can be found in Journel and Huijbregts (1978). Kriging differs from the Gandin type of OI in the way that it is usually applied to atmospheric and oceanic analyses: it is formulated in terms of an anisotropic structure function rather than the autocorrelation, and the analysis is "unbiased" in that it preserves the average value of the observations, whereas the usual Gandin approach leads to analyses that tend to zero when data are sparse. These properties make Kriging more suitable for analysis of climatological maps. Kriging is also an exact interpolation, meaning that if an observation falls exactly on an analysis grid point, its value is returned by the analysis for that point; however, this feature is of little significance in our application.

The value of the parameter to be mapped is estimated at each mapping grid point as a linear combination of surrounding observed values; that is,

$$p_o^* = \sum_{i=1}^{n} w_i p_i \quad , \tag{1}$$

in which p_o^* is the estimated value at the point to be interpolated, p_i are the observed values at surrounding points, and w_i are weights to be selected in such a way as to obtain the "best" interpolated value. Best can be qualified in many ways. The weights used for Kriging are determined to provide estimates that have zero mean difference and minimum mean-square difference relative to the true field values. That is,

$$\langle p - p^* \rangle = 0 \tag{2}$$

and

$$\langle (p - p^*)^2 \rangle = \text{minimum} \quad , \tag{3}$$

in which the angle brackets denote mean values. Thus, Kriging produces an analysis that is optimal in the sense that it gives the correct value in the mean rather than systematically higher or lower values, and has the lowest mean-square error of any estimation scheme based on linear combinations of observed values. The method is therefore described as a best linear unbiased estimator.

Substitution of Eq. (1) into Eq. (2) leads to

$$\sum_{i=1}^{n} w_i = 1 \quad . \tag{4}$$

Similarly, substituting Eq. (1) into Eq. (3) and differentiating with respect to the coefficients w_i leads to the set of equations

$$\sum_{j=1}^{n} w_j \gamma_{ij} + \lambda = \gamma_{oi}, \quad (i = 1,2,\ldots,n) \quad , \tag{5}$$

in which λ is the Lagrange multiplier associated with minimizing (3) subject to the unbias constraint (4), and

$$\gamma_{ij} = \frac{1}{2} \langle (p_i - p_j)^2 \rangle \quad . \tag{6}$$

The function γ_{ij}, expressed as a function of the distance between points of interest, is called the variogram, but is more familiar to oceanographers and meteorologists as the structure function. It is presumed to be known or to be determinable from the data to be analyzed, for all parts of the data field. As a practical matter it is assumed that a single structure function is appropriate to all parts of the field.

A useful feature of the method is that, together with the field of estimated values, it provides a complementary map of the "Kriging variance" σ_k^2, that is, the mean square uncertainty of the analysis:

$$\sigma_k^2 = \langle (p - p^*)^2 \rangle = \sum_{i=1}^{n} w_i \gamma_{oi} + \lambda \quad . \tag{7}$$

In our application, σ_k represents errors of observation, within season and interannual (among relatively normal years), and the regional distribution of observations.

Software packages are commercially available to perform the matrix operations implied in Eqs. (1)-(7). For this work we used KRIGPAK subroutine GKRIG2. KRIGPAK is a UNIRAS Corporation product. Determination and mathematical representation of the structure functions were done using routines developed by the authors.

The importance of the structure function is evident from Eqs. (5) and (7). The structure functions used in our analyses were computed from the data fields to be analyzed. Squared point-value differences were averaged by 1° latitude or 2° longitude intervals of separation distance, the first interval

Table 2.—Structure function model parameters

Isotherm (C)	a (m^2)	10^4b (m)	y'/y
20°	120	2.66	3.41
15°	360	2.68	4.24
10°	550	1.44	7.30

having 0.5° to 1.5° or 1° to 3° separation, etc. Pairs lying within 5° of east-west or north-south orientation were accepted in forming the averages. Because of the predominantly zonal nature of the tropical currents and density pattern, the structure function is strongly anisotropic, rising more rapidly in the north-south than in the east-west direction. The GKRIG2 routine allowed only for use of a radial structure function, so it was necessary to represent the structure functions in the two directions in similar functional form and to bring them into coincidence by rescaling. The data fields also had to be scaled for the interpolation and restored to proper scale for the mapping.

We first computed the directional structure functions for each of the three isotherm depths and four seasons. No systematic differences appeared among the four seasons, so all of the values for each isotherm depth were merged to obtain a more stable and reliable result. The structure function in the east-west direction was reasonably linear for lags of up to about 20°, beyond which it became erratic due to relatively small numbers of data pairs. In the north-south direction the structure functions were reasonably linear for only half this distance or less. A linear least-squares fit was made in each direction, the zero-lag intercepts were averaged, and the ratio of slopes was used to determine the required coordinate stretch. Table 2 contains a summary of parameters a and b for a structure function model of the form

$$\gamma(\ell) = a + b\ell \quad , \tag{8}$$

in which separation ℓ is measured in meters. The column y'/y in Table 2 denotes the scale distortion required in the analysis. The structure function models are displayed in Fig. 5 in relation to the experimental values on which they are based.

The Kriging equations [(1), (5)] were used to obtain estimates of the isotherm depths and Kriging standard deviations (rms error estimate) at 2° grid point intervals in the region 20°N-20°S and from 140°W to the coast of Central and South America. These results were then plotted and contoured by computer. The numerical results displayed on shaded contour maps are presented after Sec. 5. Each pair of maps shows the estimated seasonal isotherm depth climatology, and its estimated rms deviation σ_k, both in meters. Each value was interpolated from the 12 or less nearest observed values within a search radius of 20° longitude, or its equivalent in stretched latitude. The interpolation was not made unless at least three observations were available within the maximum search radius.

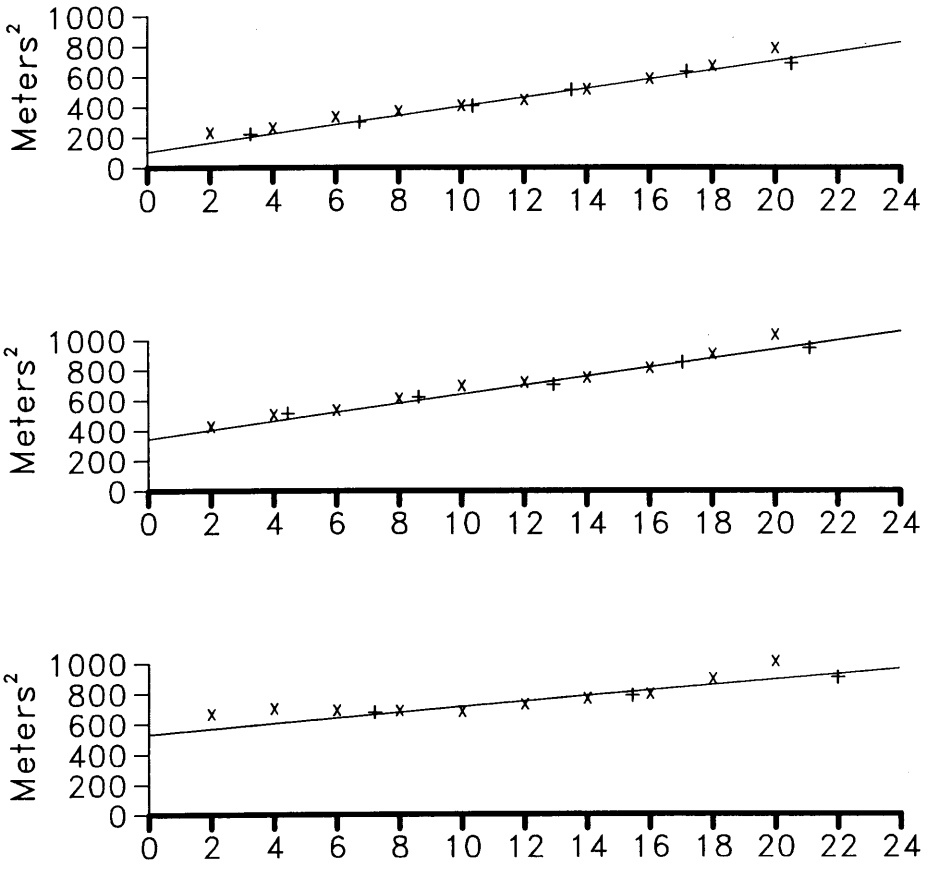

Figure 5.--Structure functions used for optimum interpolation of the depths of 20°C (top), 15°C (center), and 10°C (bottom) isothermal surfaces, based on experimental values in the zonal direction (×) and in the meridional direction (+).

In regions where the deviation exceeded 25 m, 30 m, and 35 m respectively for the depths of the 20°C, 15°C, and 10°C isotherms, the analyses were thought to be more misleading than useful, so the results from these regions were deleted from the final maps.

4. DISCUSSION

Two kinds of comparison were made to evaluate the utility of this product. For the first comparison, we mapped the differences between the depth of the 15°C isotherm in this climatology and that of Levitus (1982) to investigate whether they were sufficient to merit publication of a new climatology. The general features of these two climatologies are, of course, quite similar, but the Levitus atlas has the 15°C isotherm systematically deeper, especially during winter, because of the inclusion of data from years during which El Niño events are known to have occurred.

For summer the differences were typically about half the local σ_k, or half our contour interval. The largest differences were found near 0°, 120°W and

20°S, 100°W, where the Levitus climatology was about σ_k deeper and shallower, respectively.

For fall the 15°C isotherm is deeper in the Levitus climatology almost everywhere, but mostly by $\sigma_k/2$ or less. Differences exceeded σ_k only along part of the southern boundary and near 10°S, 133°W.

The largest differences were found for winter, in which the Levitus depths exceed ours in a broad band along 5°N-10°S, ranging from $2\sigma_k$ at the western boundary to about σ_k east of the Galapagos Archipelago. During this season the depths in the Levitus climatology are less than ours only in the northwest and southeast sections of the mapped region, and by only about $\sigma_k/2$ or less.

The greatest variability between these climatologies was found during the spring. The Levitus climatology shows the influence of data from historic El Niño events; its 15°C isotherm is deeper over much of the region, having a maximum of $2\sigma_k$ at the coast of Ecuador. But that isotherm is also nearly $2\sigma_k$ shallower near 10°N, 125°W and 20°S, 95°W.

The Levitus climatology is consistently shallower than ours along the coast of Peru south of about 15°S. Our data were inadequate to give any con fidence in the analyses for this region. It is the principal region in which results were deleted from the maps because of large σ_k values. We have not investigated the quality of the Levitus climatology for this region, but expect that Levitus' resolution, like ours, is inconsistent with the gradients in this strong coastal upwelling area.

For the second comparison, we computed isotherm depth anomalies from observations that were made during 1979 and early 1980 and that were not used in construction of the climatology. There were some indications of El Niño/ Southern Oscillation anomalies in the western tropical Pacific during 1979 (Donguy et al., 1982), but these anomalies did not develop in a typical fashion; an El Niño event was not recognized in the eastern Pacific although substantial weather and oceanographic observations were made in connection with the Global Weather Experiment. Isotherm depths during 1979-1980 were found to be deeper than our climatology showed, particularly along the equator and in the region of the South Equatorial Current, but by modest amounts of about $1\sigma_k$, and only isolated values of up to $2\sigma_k$. Negative anomalies appeared in the region of the North Equatorial Countercurrent. The average anomalies and their variations over the mostly near-equatorial and eastern boundary observations available were about $\sigma_k/3$ and $2\sigma_k/3$ respectively. These values indicate slight deepening of the isotherms in the eastern equatorial Pacific, but corroborate the judgment of the time that conditions did not warrant identification as El Niño.

A final question of some importance is that of the quantitative significance of our σ_k maps. They are determined in significant part by the structure functions, which are assumed to be representative of the entire fields and all seasons at each level. To test the relationship between the σ_k fields and the uncertainty of the analyses, we applied a form of cross validation. At each observation point the observed value was removed from the data and its value interpolated from the surrounding values. The root-mean-square difference between the values so estimated and the actual observation was calculated for each field and divided by the average value of σ_k over the field. In no case did the rms difference differ from σ_k by more than 15%, and the overall average of their ratio was 1.01 ± 0.03. We conclude that the σ_k maps are a quantitative measure of the variability inherent in our data and analyses.

5. REFERENCES

Clark, I., 1979. Practical Geostatistics. Applied Science Publishers, Essex, England, 129 pp.

Donguy, J.-R., C. Henin, A. Morlieri, and J. P. Rebert, 1982. Appearances in the western Pacific of phenomena induced by El Niño in 1979-80. Trop. Ocean-Atmos. Newsl. 10:1-2.

Gandin, L. S., 1963. Objective Analysis of Meteorological Fields. Translated from the Russian by Israel Program for Scientific Translation, Jerusalem, 1965 (available from National Technical Information Service, Springfield, VA, TT 65-50007), 184 pp.

Journel, A. G., and C. S. Huijbregts, 1978. Mining Geostatistics. Academic Press, New York, 600 pp.

Levitus, S., 1982. Climatological atlas of the world ocean. NOAA Professional Paper 13, Rockville, MD, 173 pp.

Love, C. M., 1971. EASTROPAC atlas. Circular 330, National Marine Fisheries Service, Washington, DC, 3 vols. (no pagination).

SIO (Scripps Institution of Oceanography), 1961. Step I expedition data report. SIO Reference 61-9, La Jolla, CA, 48 pp.

Tsuchiya, M., 1974. Variation of surface geostrophic flow in the eastern tropical Pacific Ocean. Fish. Bull. 72:1075-1086.

MAPS OF ISOTHERM DEPTHS

The following twelve pairs of maps present the seasonal climatological depths of the 20°C, 15°C, and 10°C isothermal surfaces, and the associated Kriging standard deviations σ_k, from 20°N to 20°S and 70°W to 140°W. The maps were obtained by optimum interpolation of data from the stations shown in Figs. 1-4. All depths are in meters.

RMS DEVIATION (σ_k), METERS

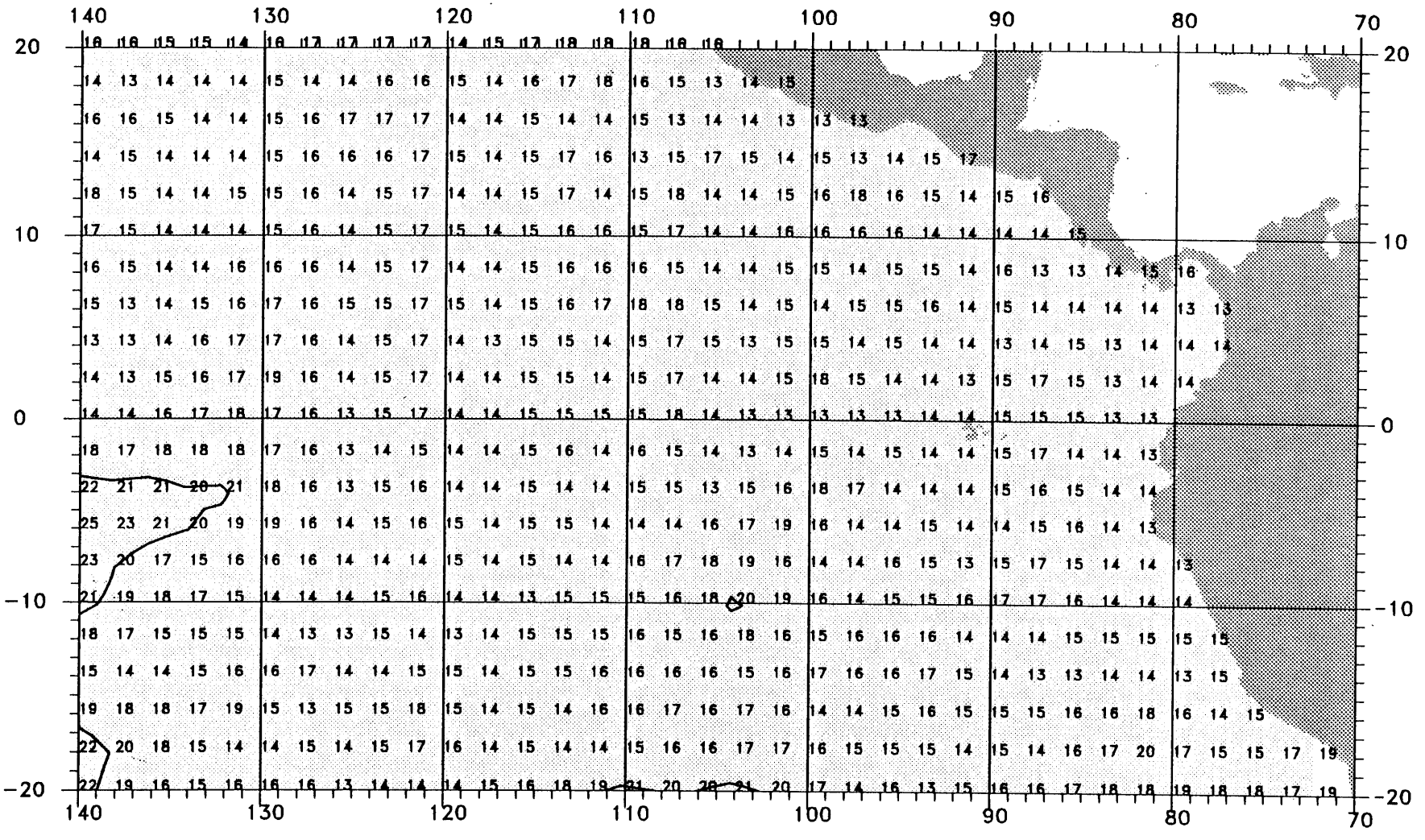

WINTER, 20° C

MAP 1a

20° ISOTHERM DEPTH, METERS

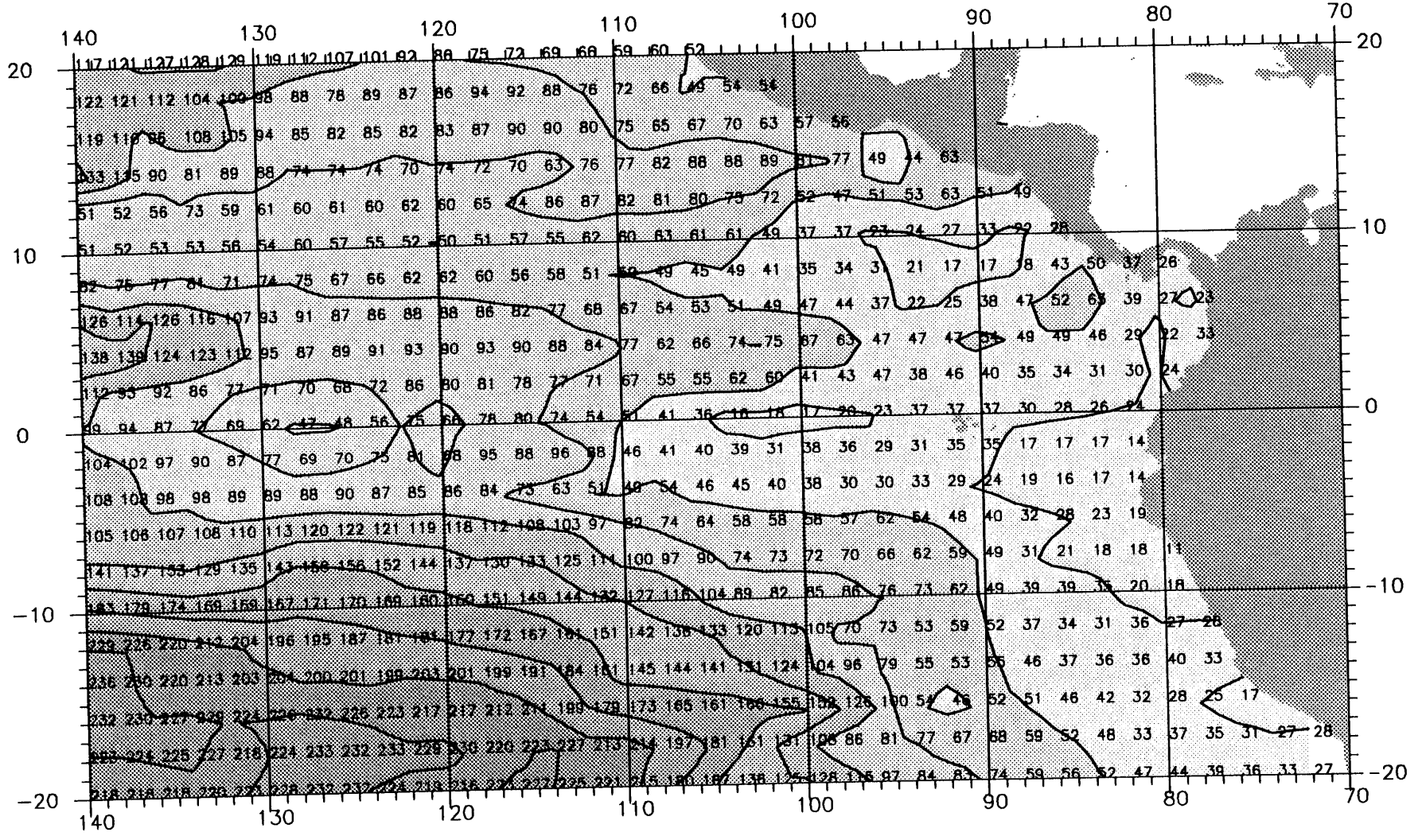

MAP 1b

RMS DEVIATION (σ_k), METERS

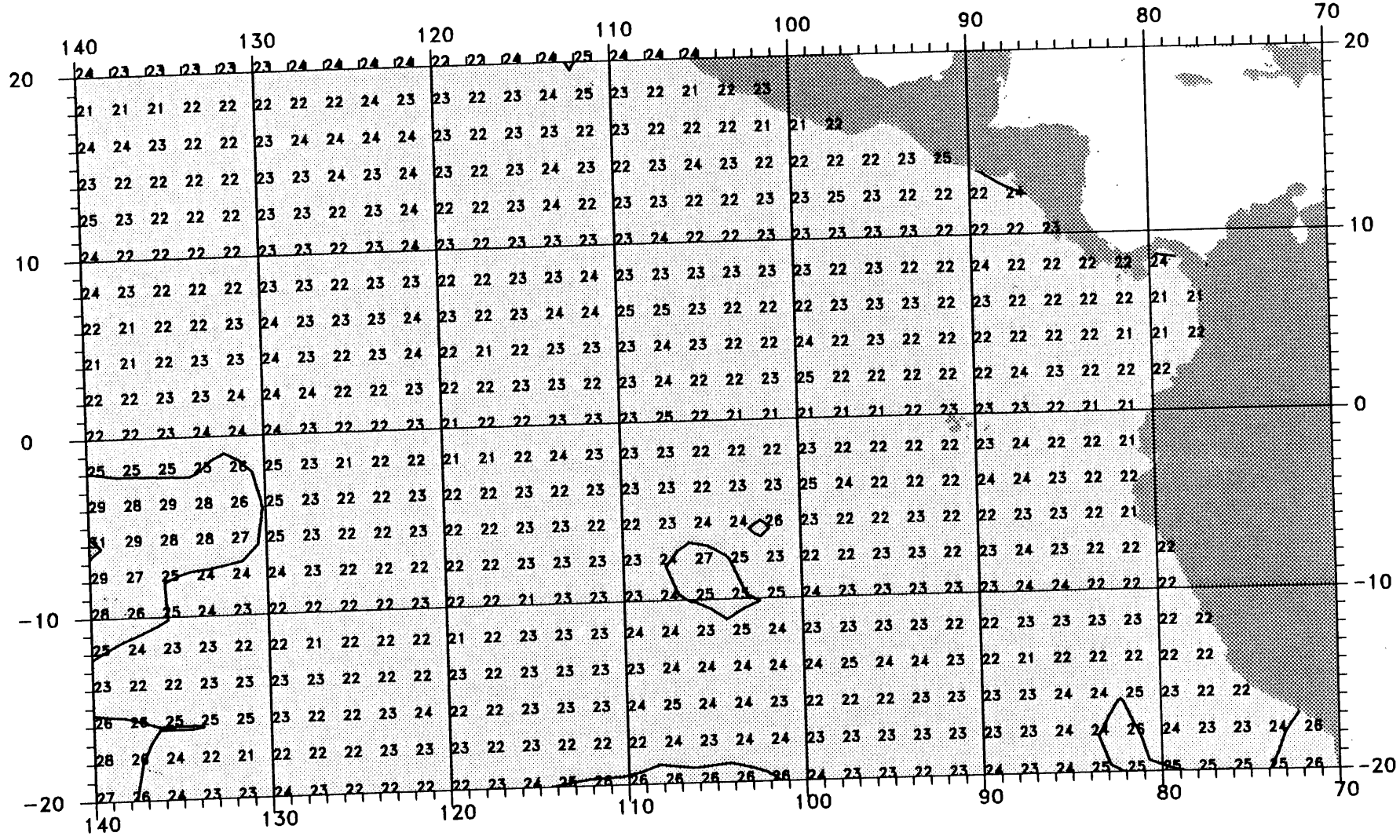

WINTER, 15° C

MAP 2a

15° ISOTHERM DEPTH, METERS

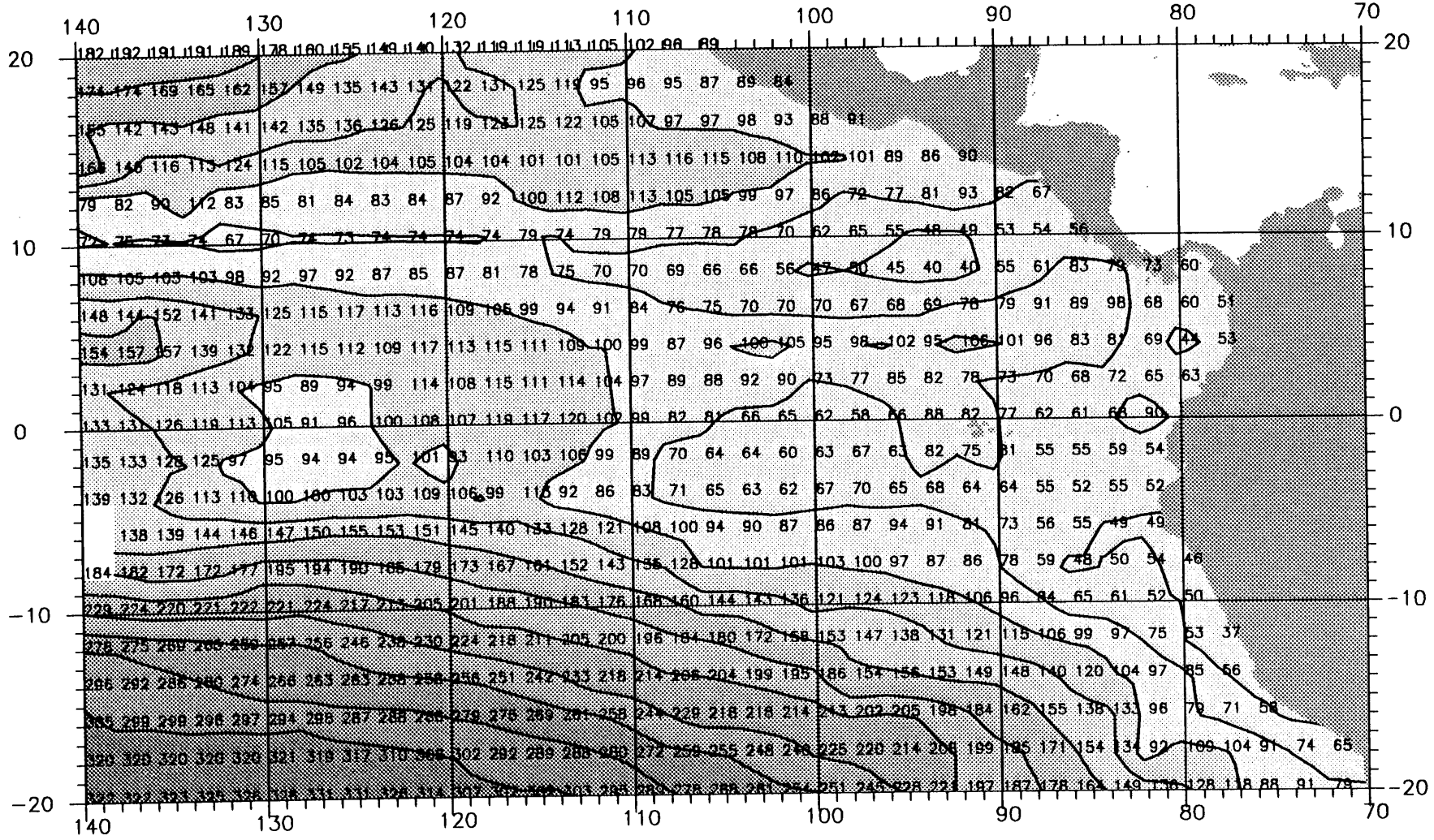

WINTER

MAP 2b

RMS DEVIATION (σ_k), METERS

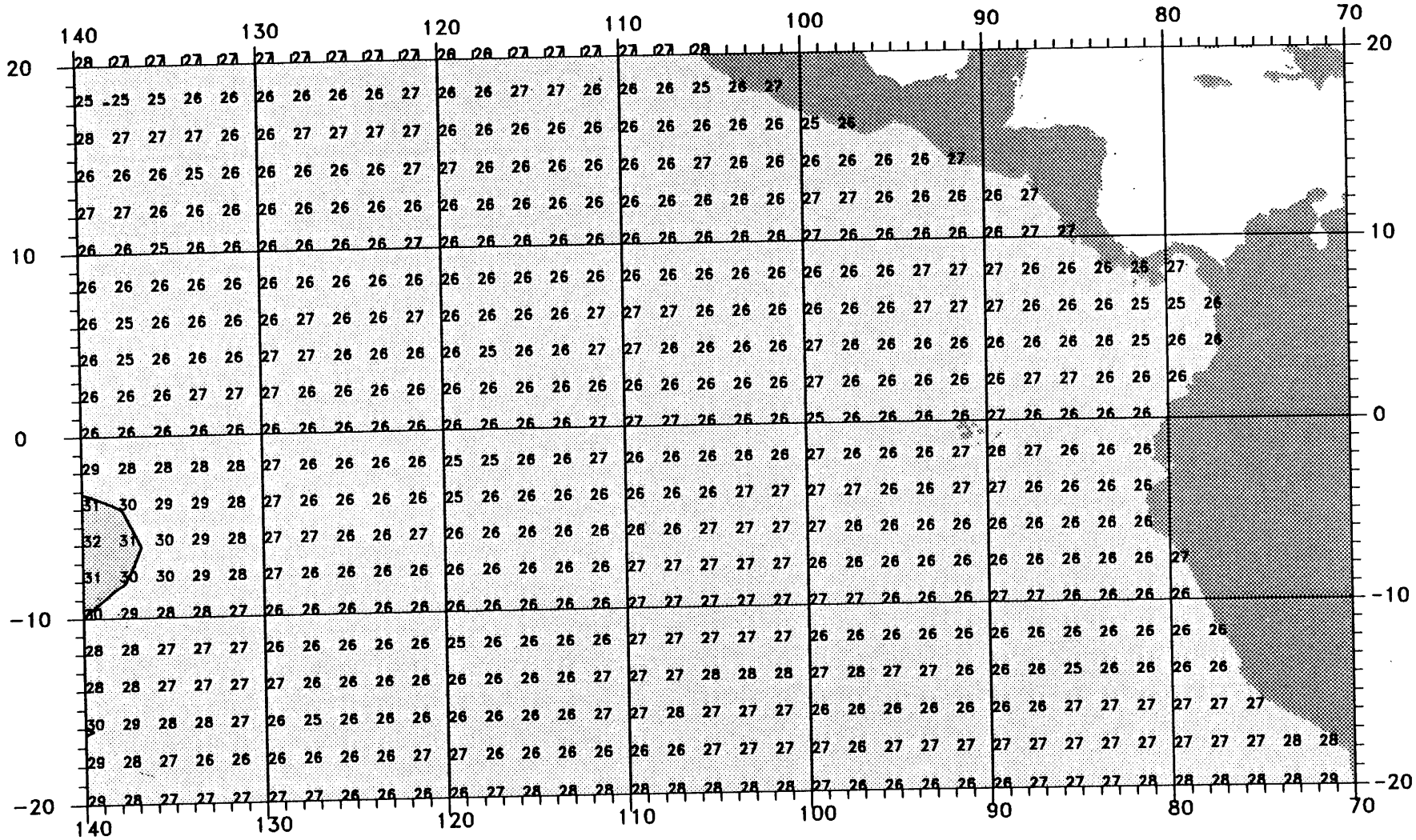

WINTER, 10° C

MAP 3a

10° ISOTHERM DEPTH, METERS

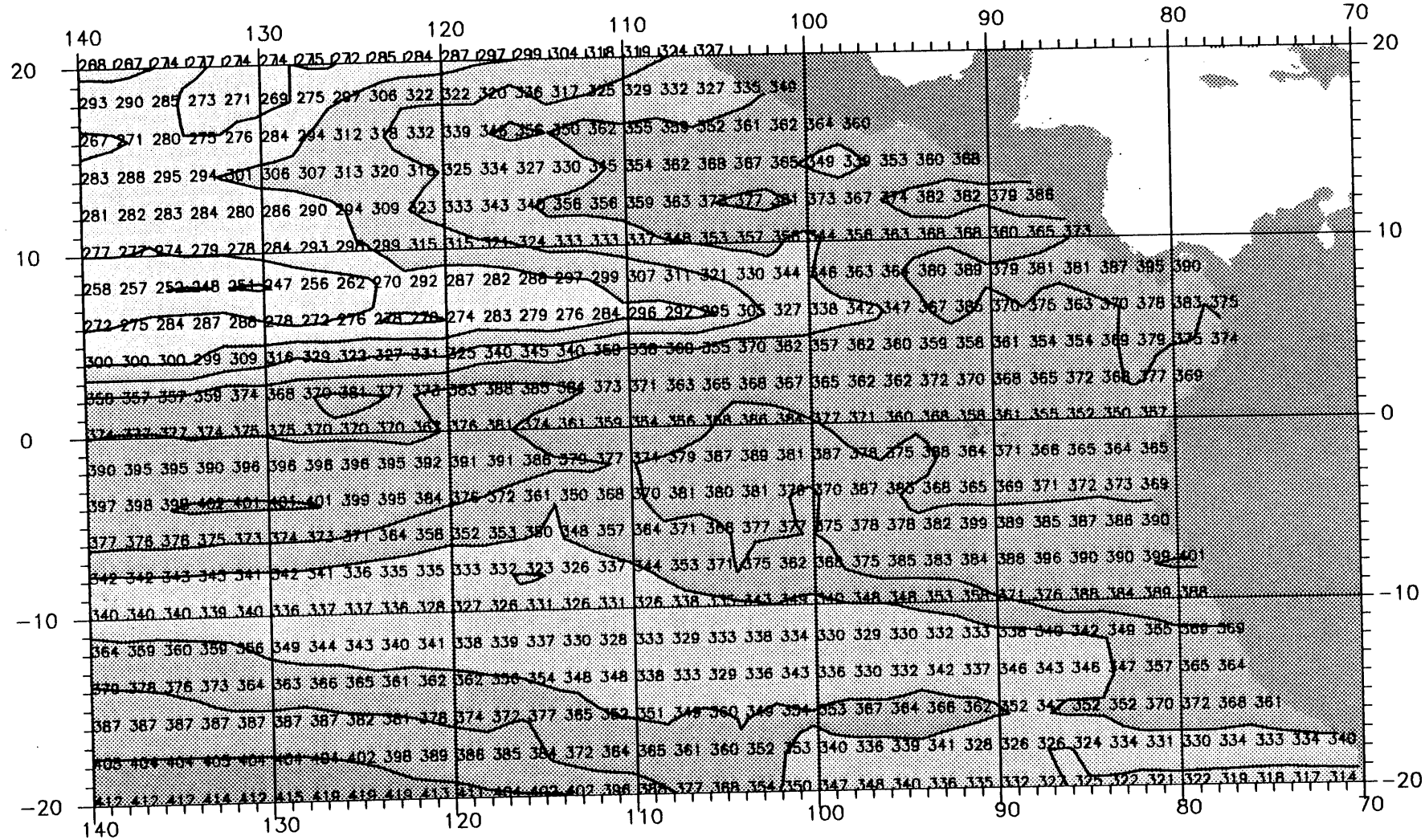

WINTER

MAP 3b

RMS DEVIATION (σ_k), METERS

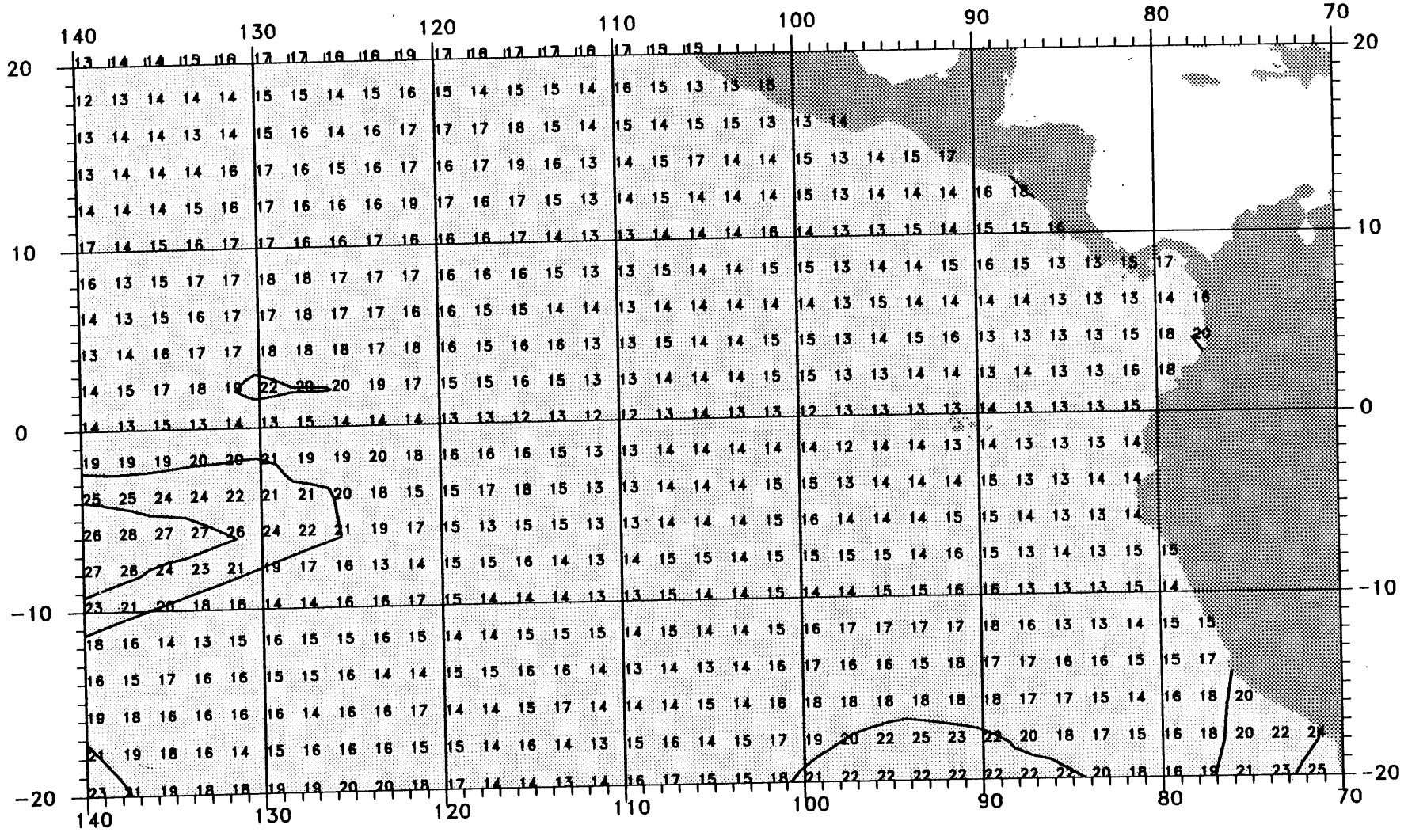

SPRING, 20° C

MAP 4a

20° ISOTHERM DEPTH, METERS

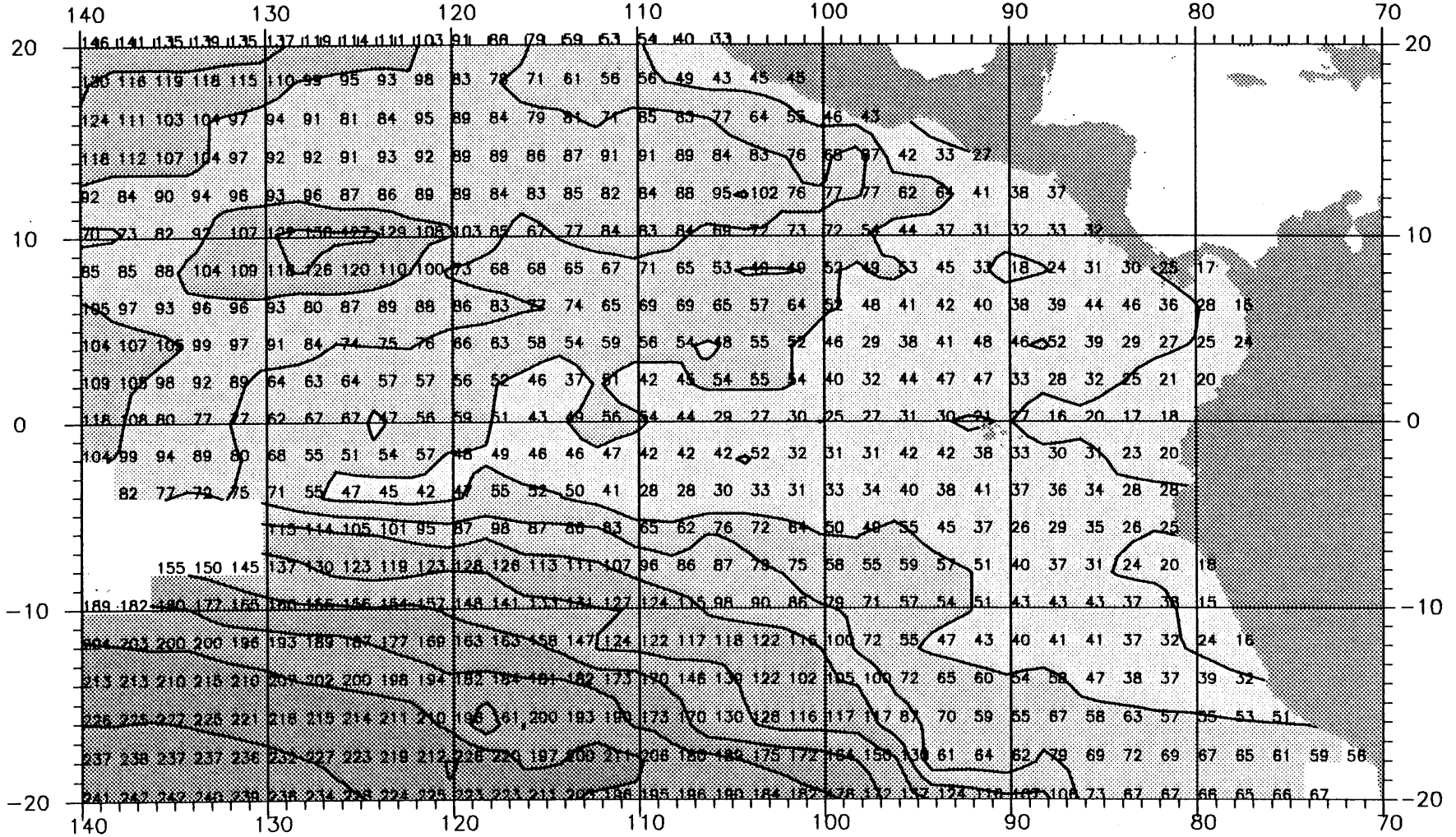

SPRING

MAP 4b

RMS DEVIATION (σ_k), METERS

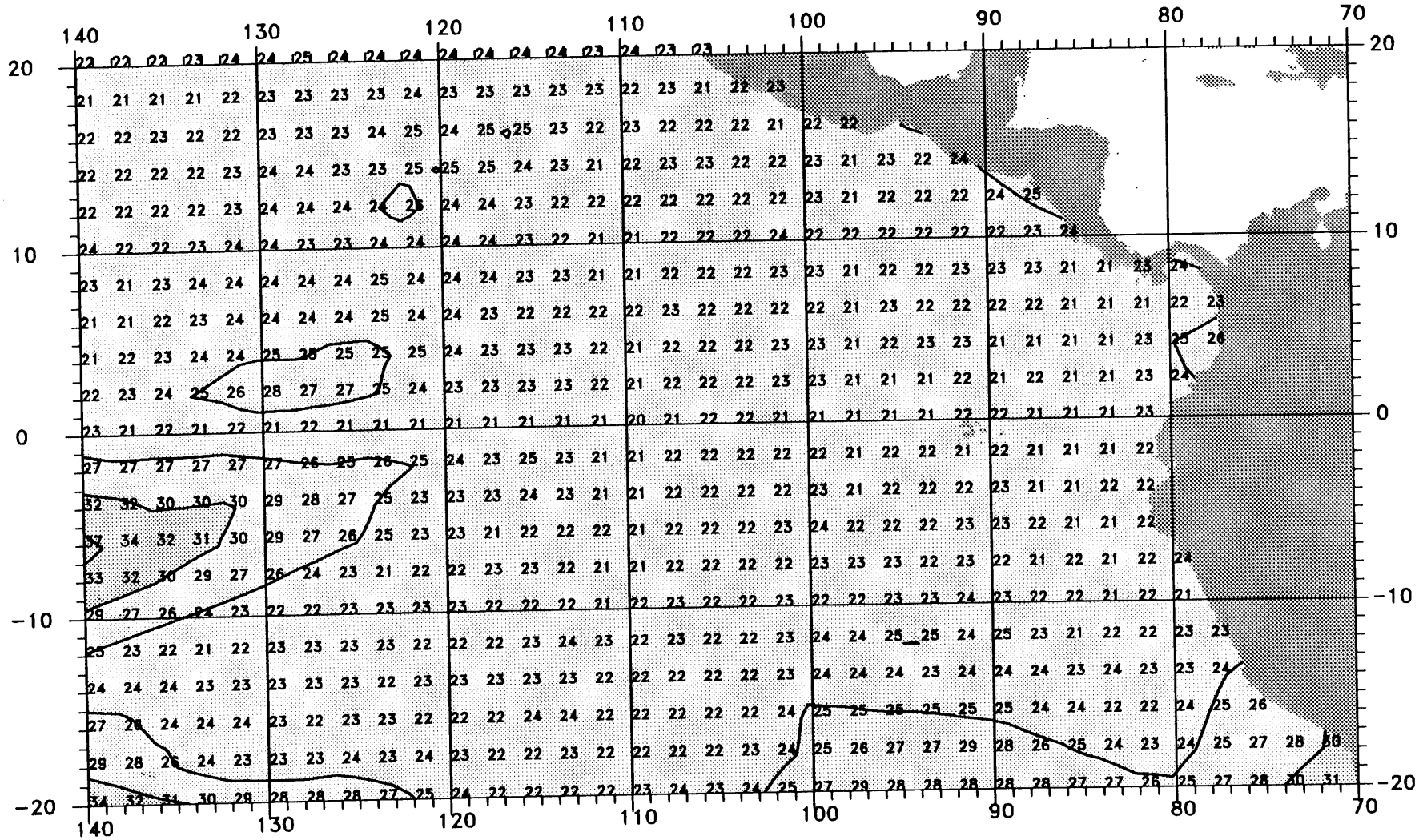

SPRING, 15° C

MAP 5a

15° ISOTHERM DEPTH, METERS

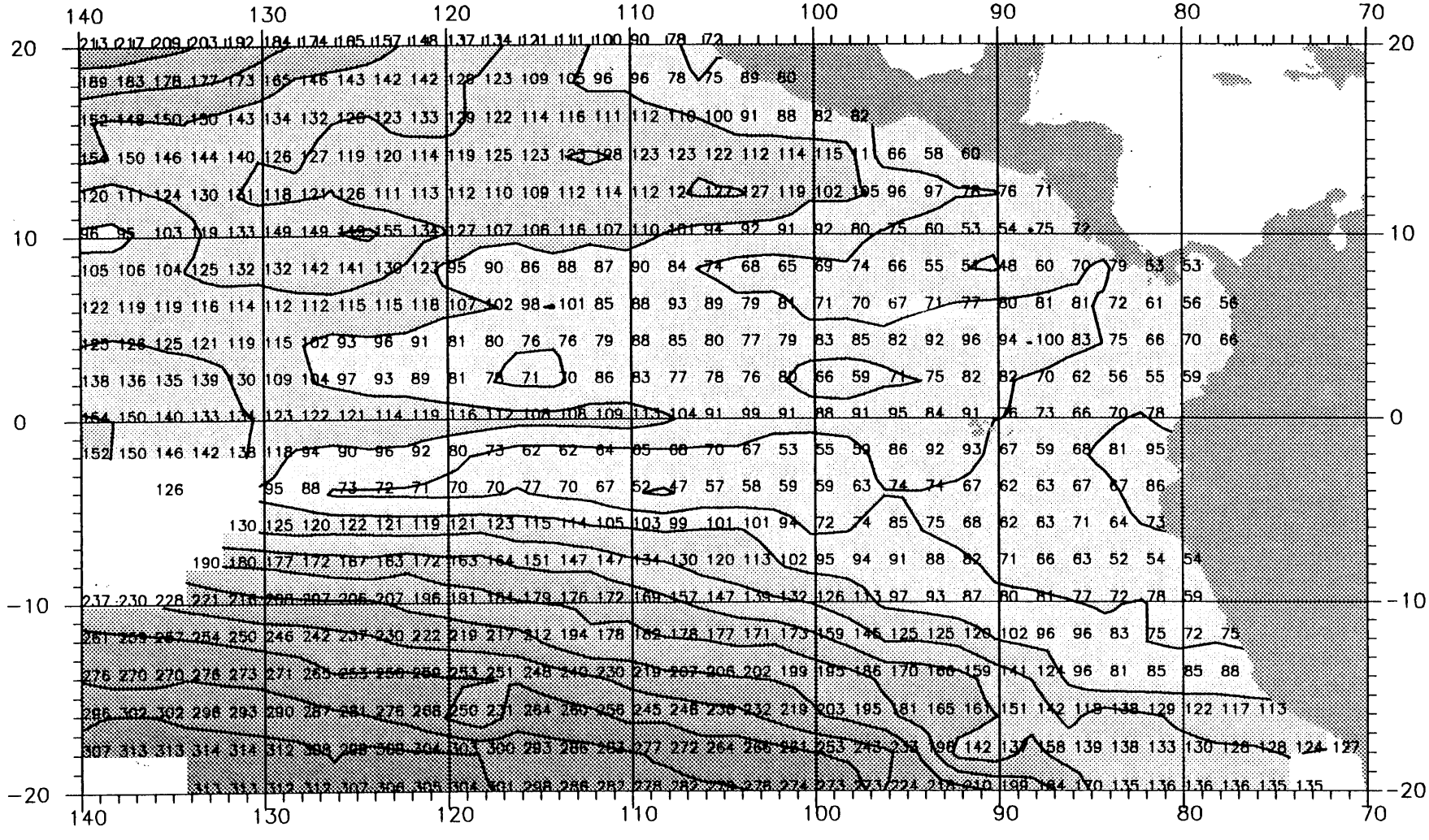

SPRING

MAP 5b

RMS DEVIATION (σ_k), METERS

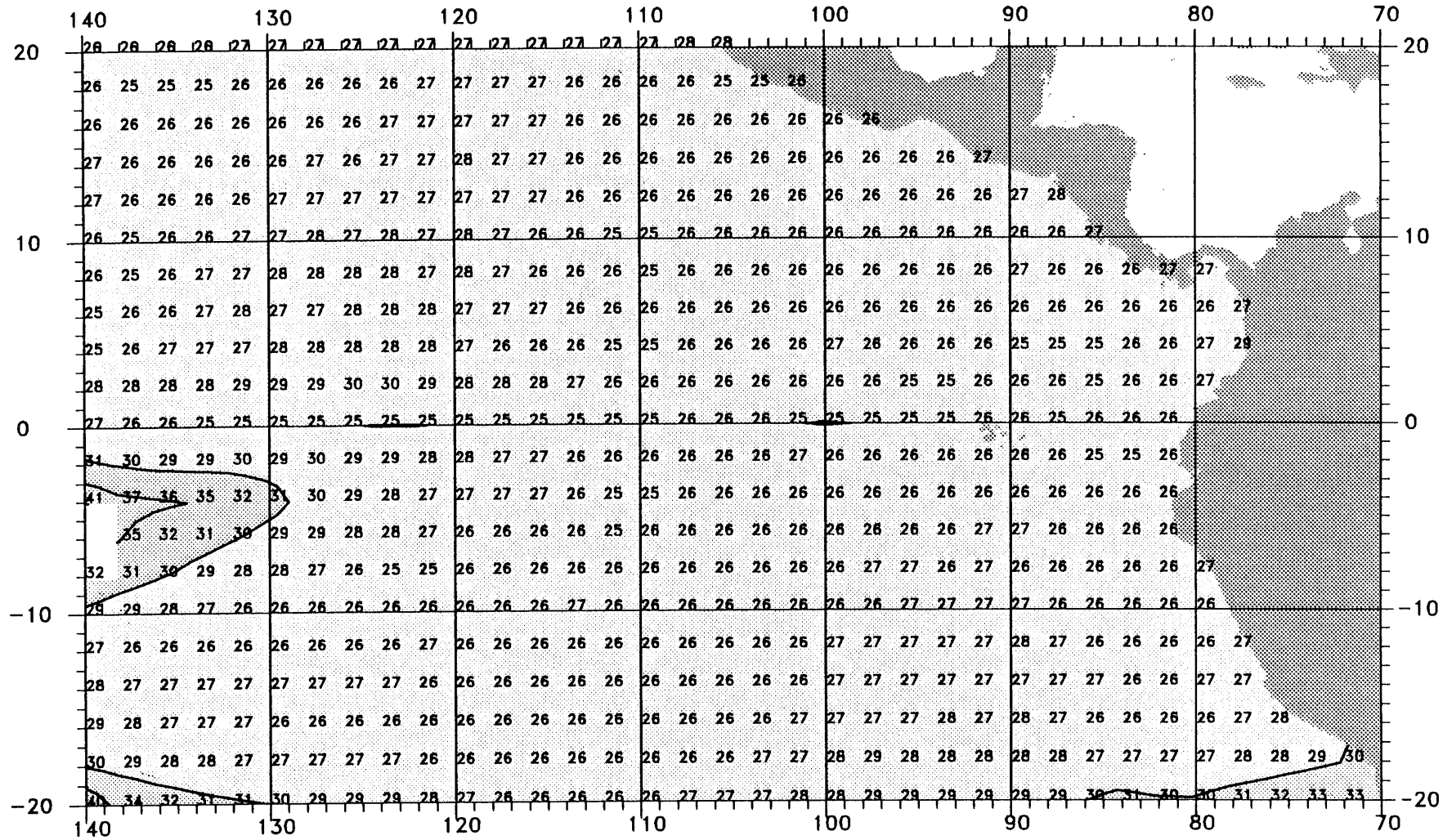

SPRING, 10° C

MAP 6a

10° ISOTHERM DEPTH, METERS

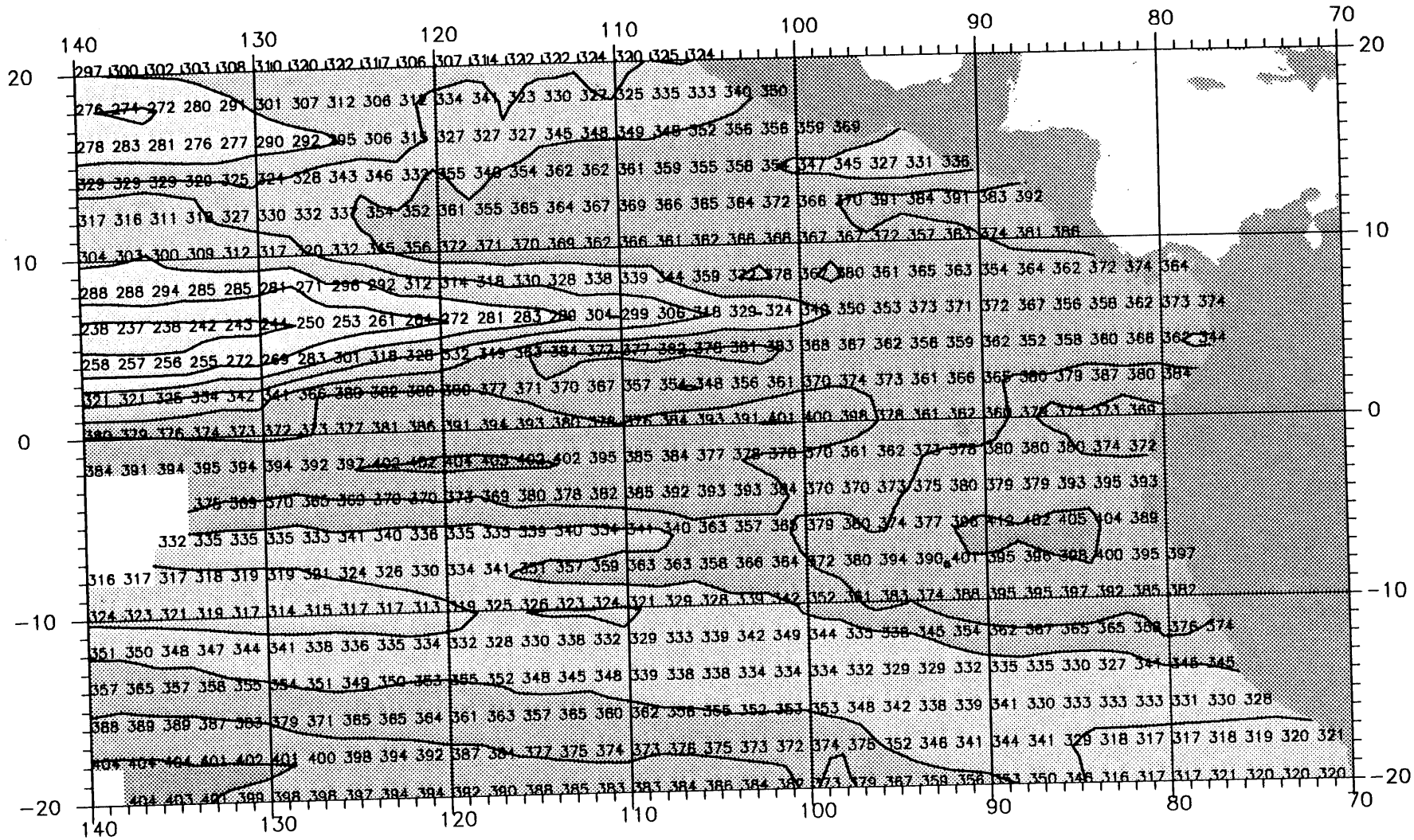

SPRING

MAP 6b

RMS DEVIATION (σ_k), METERS

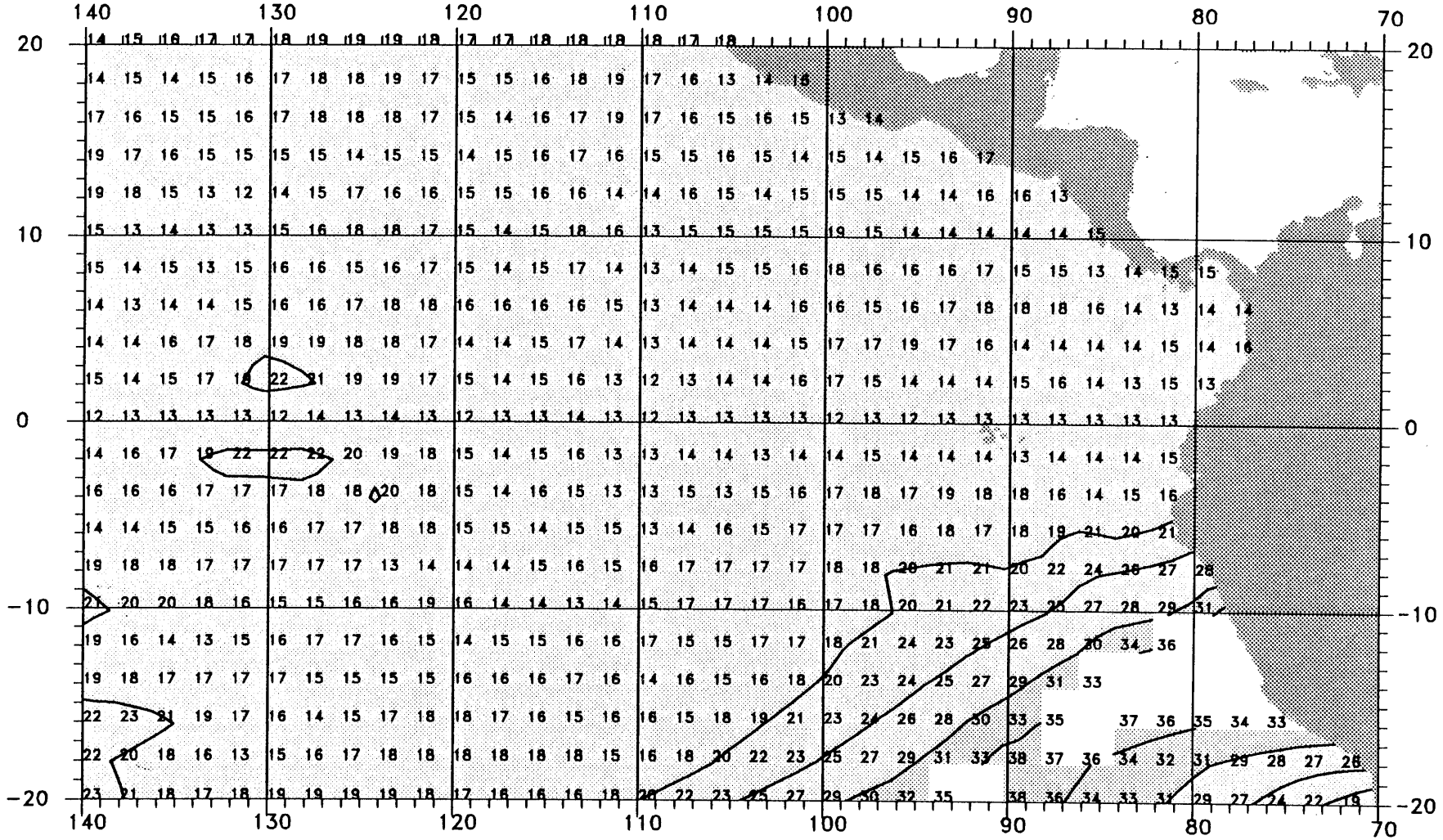

SUMMER, 20° C

MAP 7a

20° ISOTHERM DEPTH, METERS

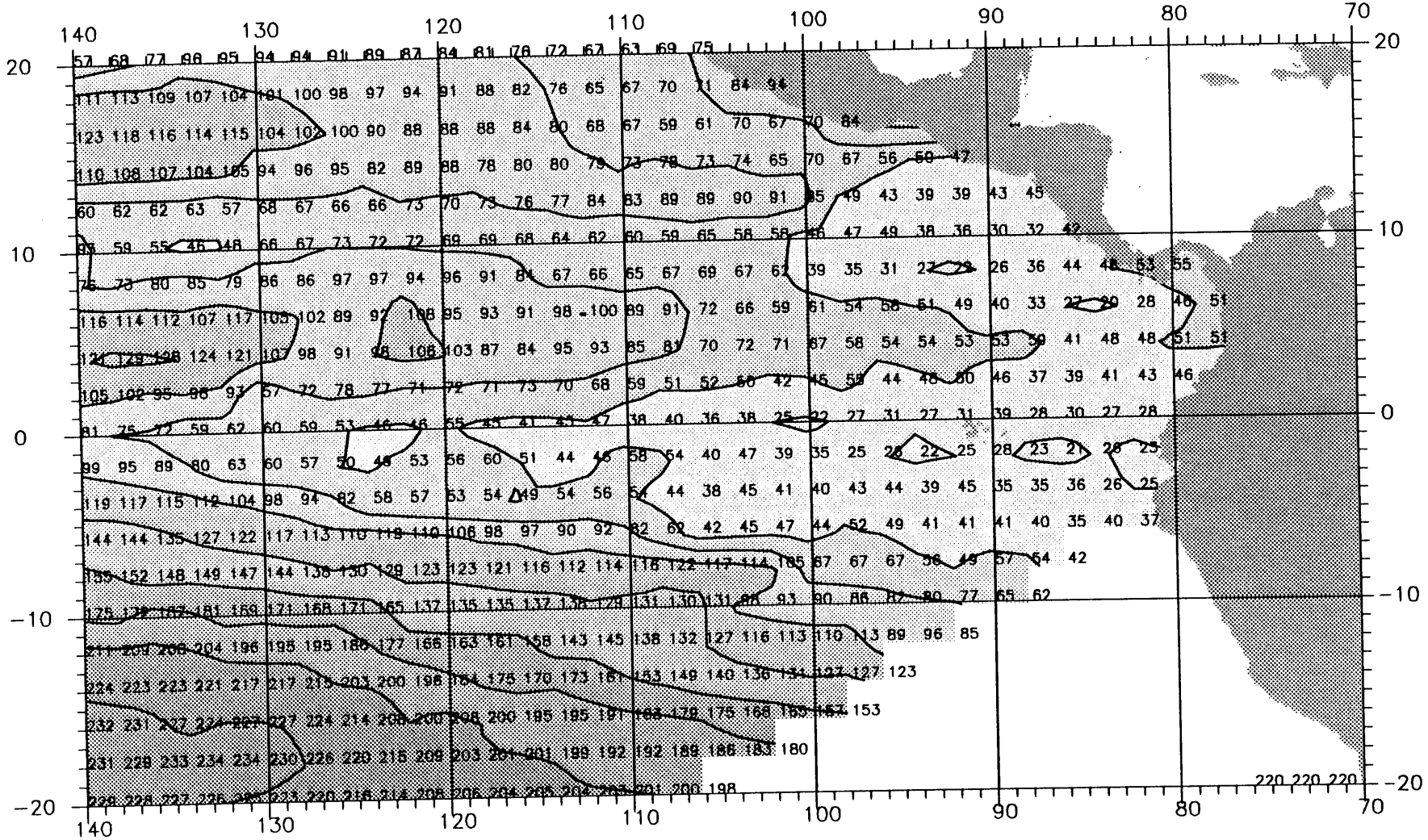

SUMMER

MAP 7b

RMS DEVIATION (σ_k), METERS

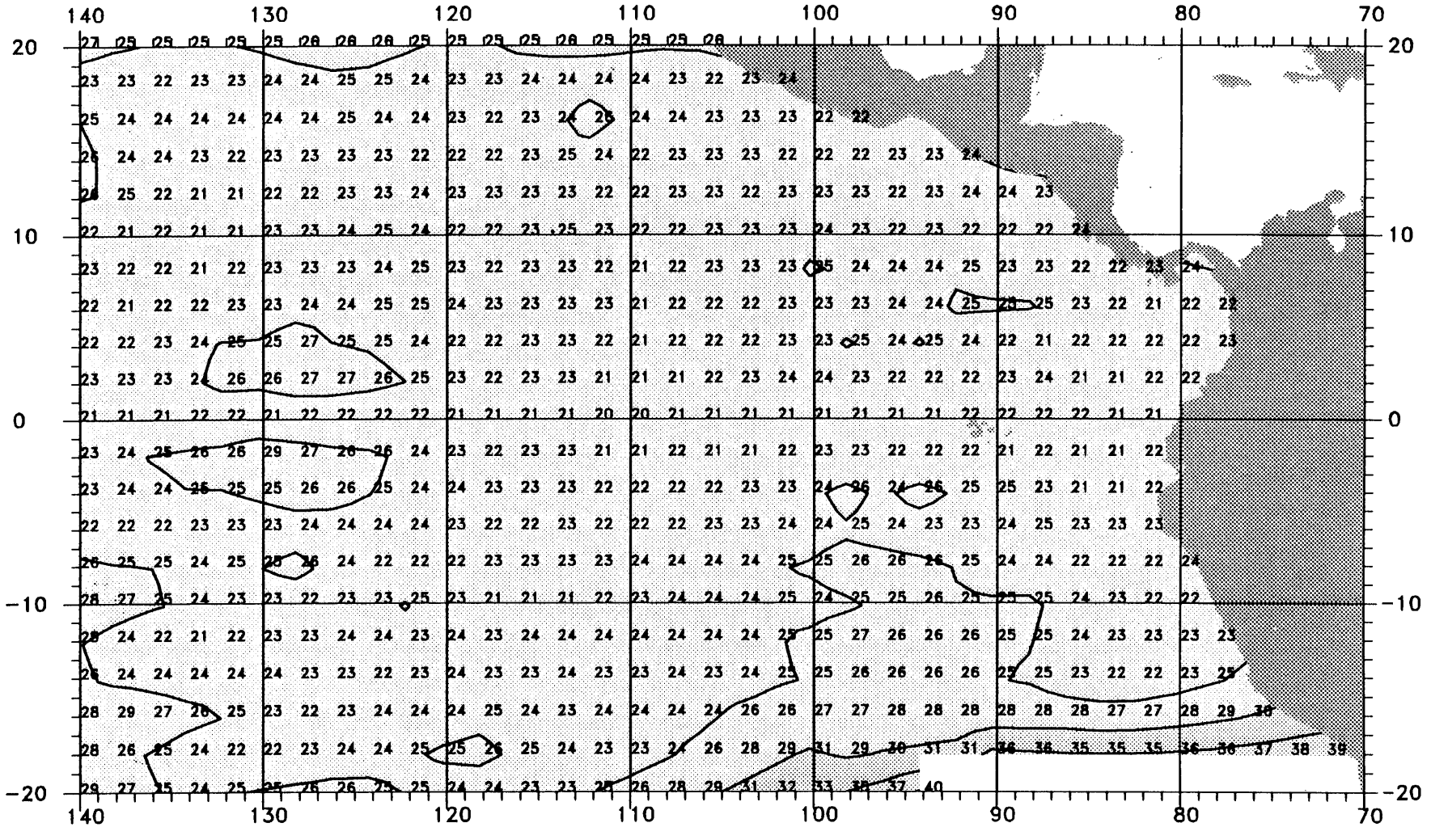

SUMMER, 15° C

MAP 8a

15° ISOTHERM DEPTH, METERS

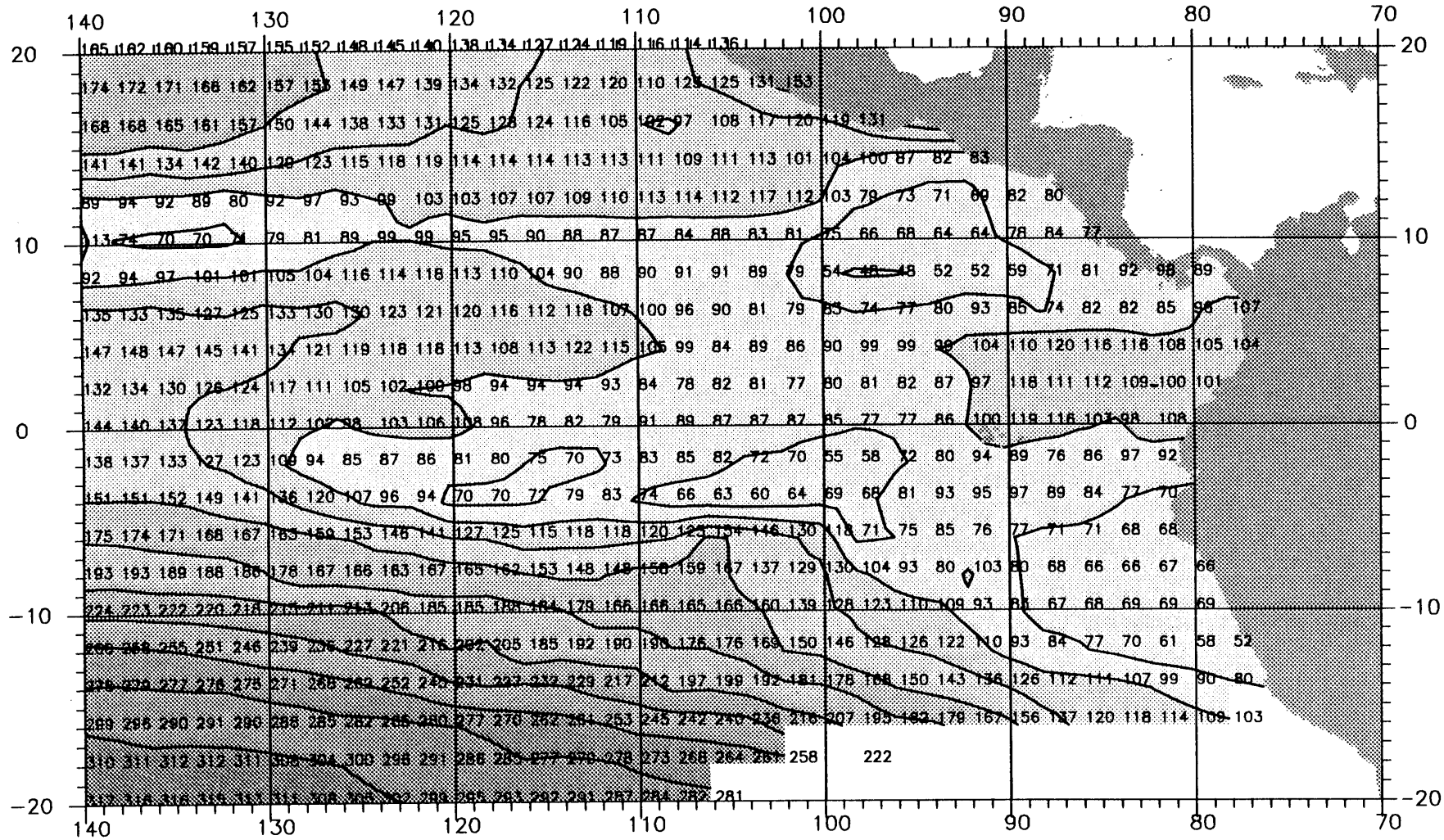

MAP 8b

RMS DEVIATION (σ_k), METERS

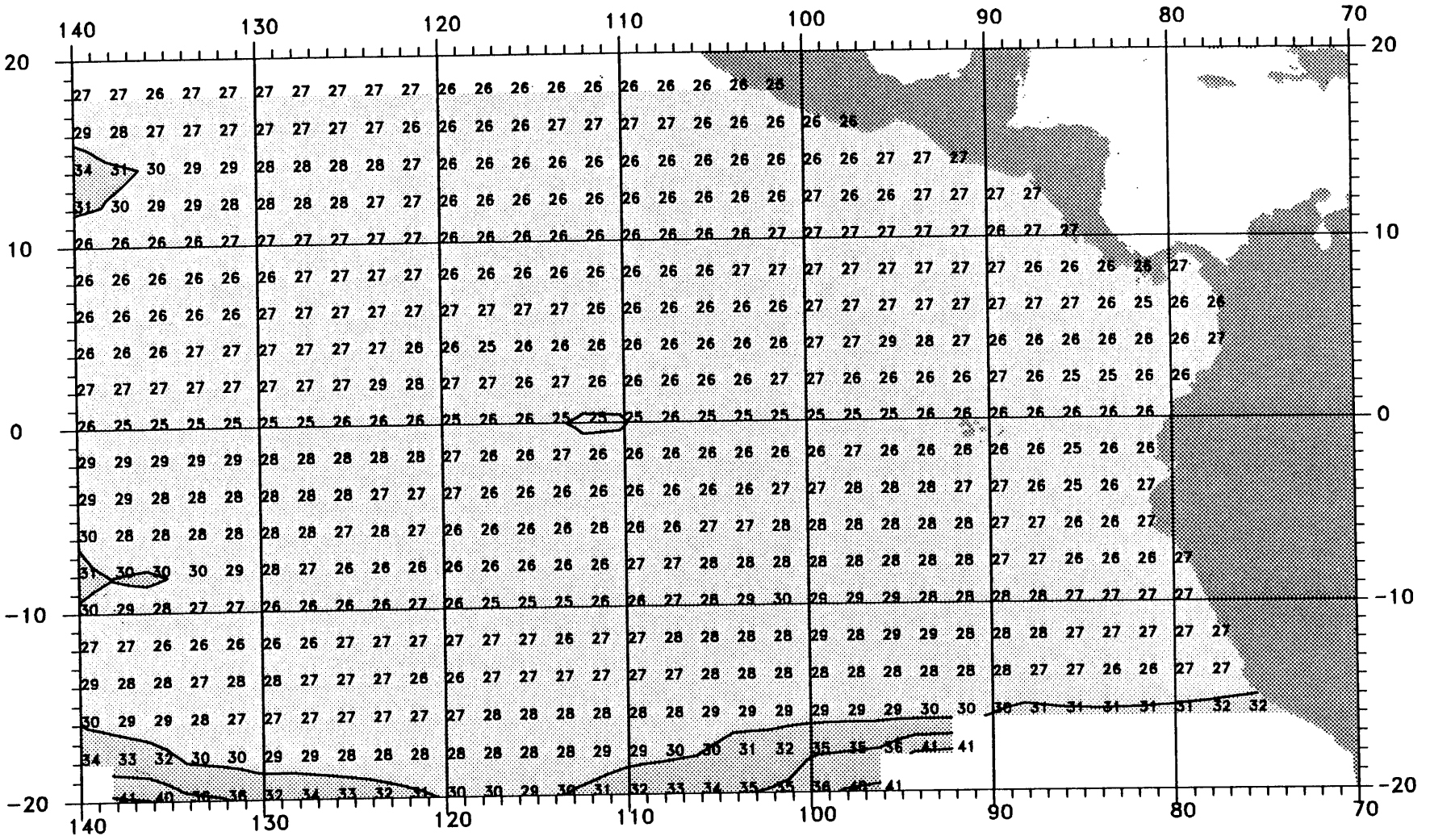

SUMMER, 10° C

MAP 9a

10° ISOTHERM DEPTH, METERS

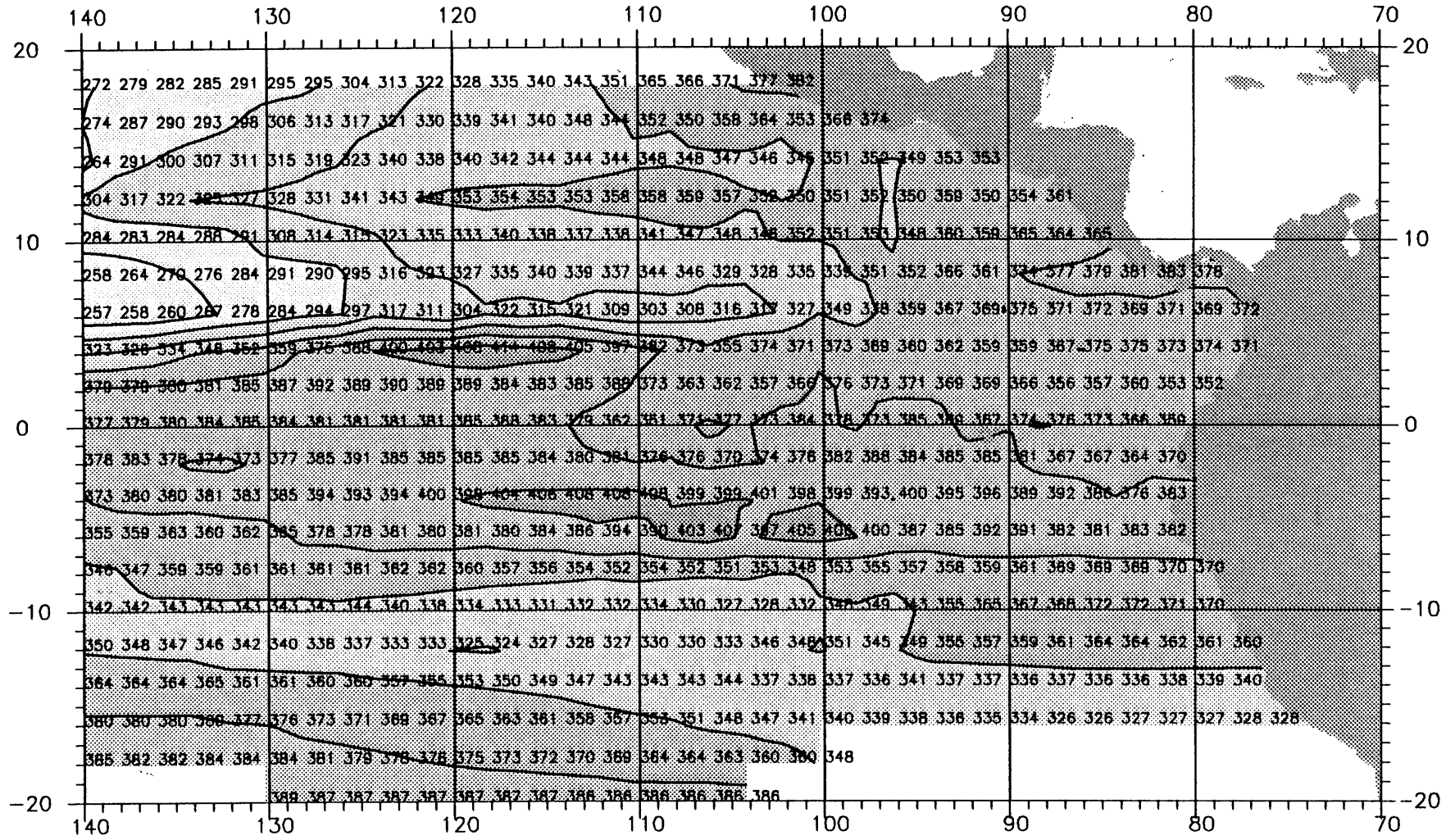

SUMMER

MAP 9b

RMS DEVIATION (σ_k), METERS

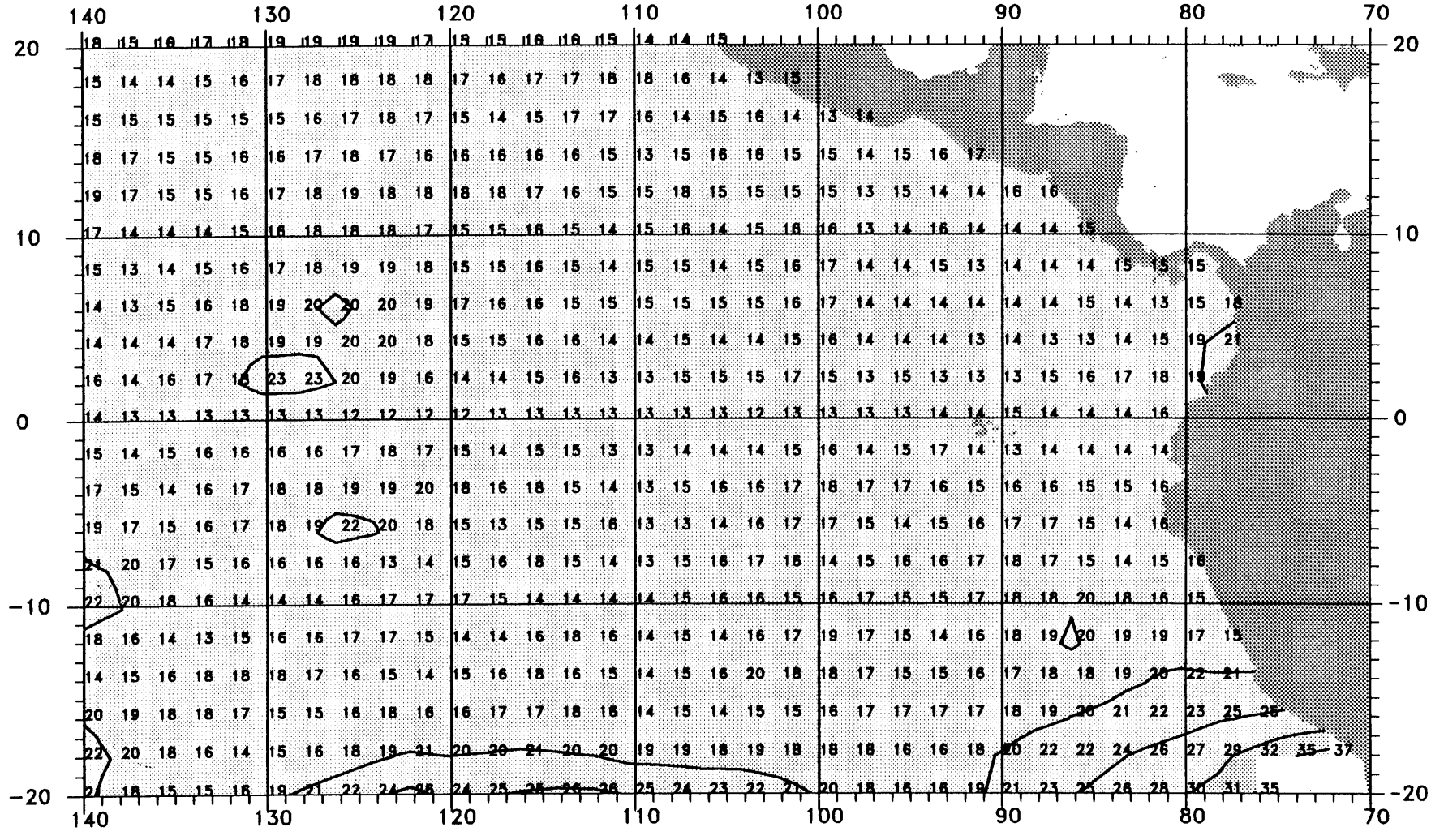

FALL, 20° C

MAP 10a

20° ISOTHERM DEPTH, METERS

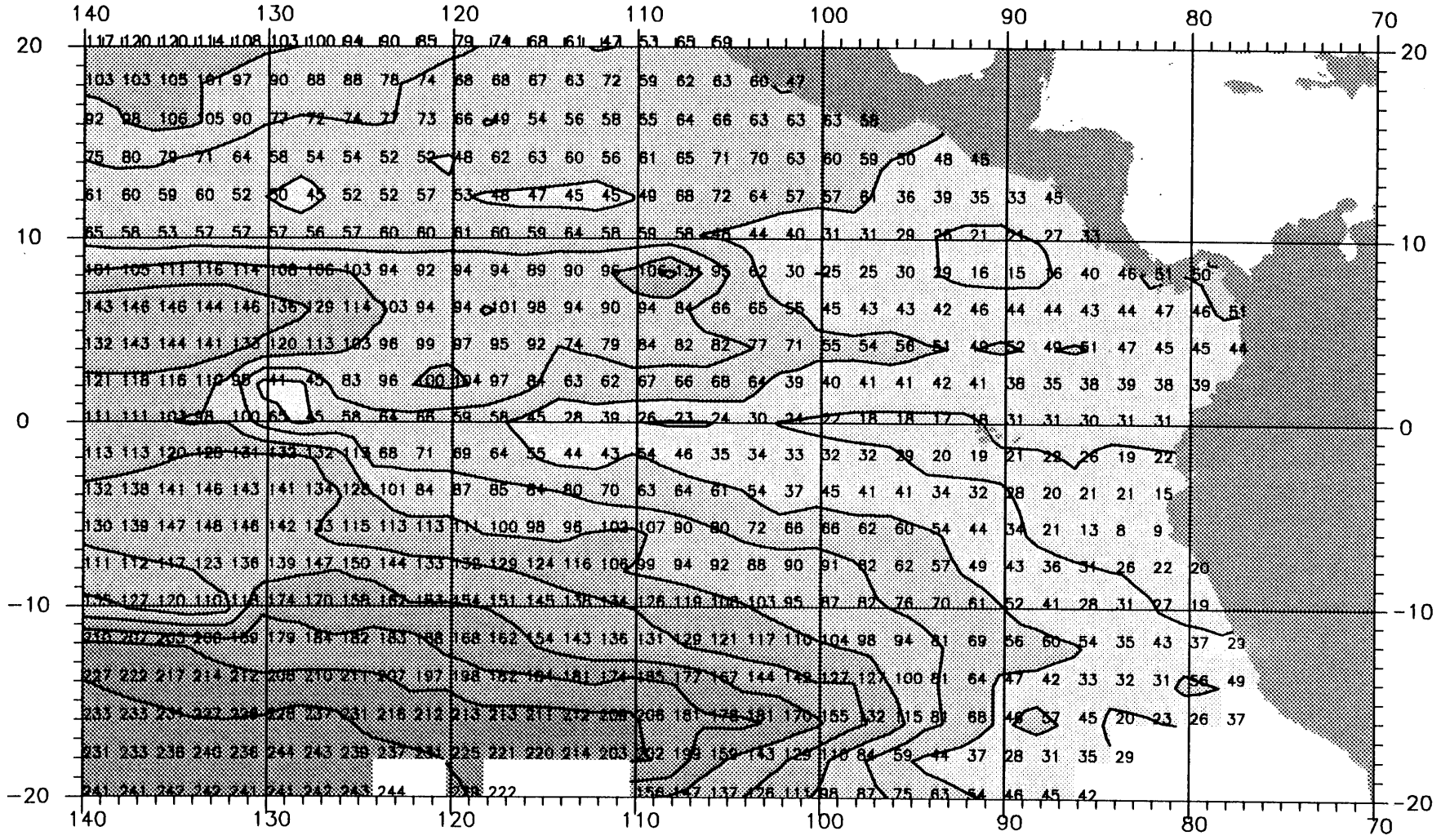

FALL

MAP 10b

RMS DEVIATION (σ_k), METERS

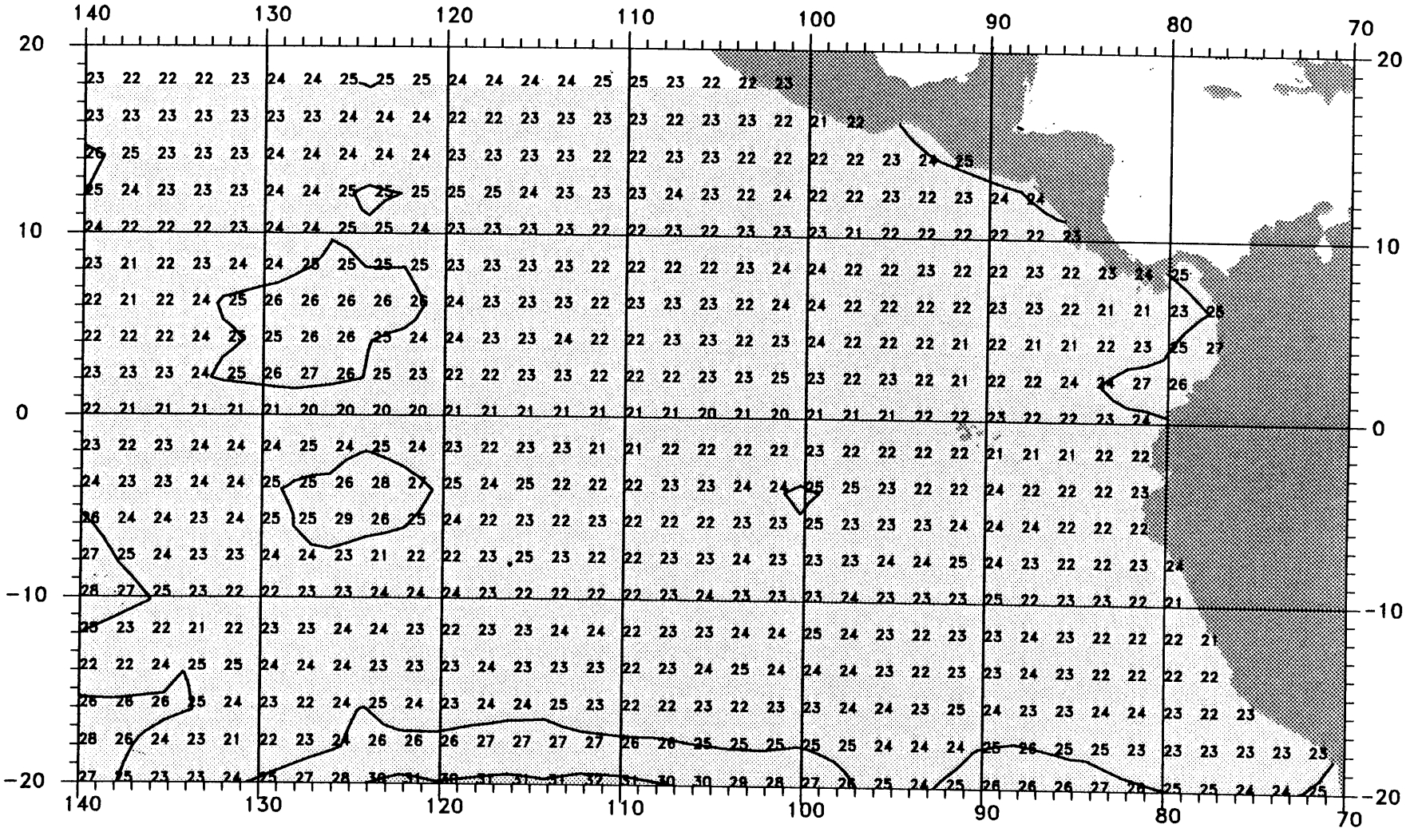

FALL, 15° C

MAP 11a

15° ISOTHERM DEPTH, METERS

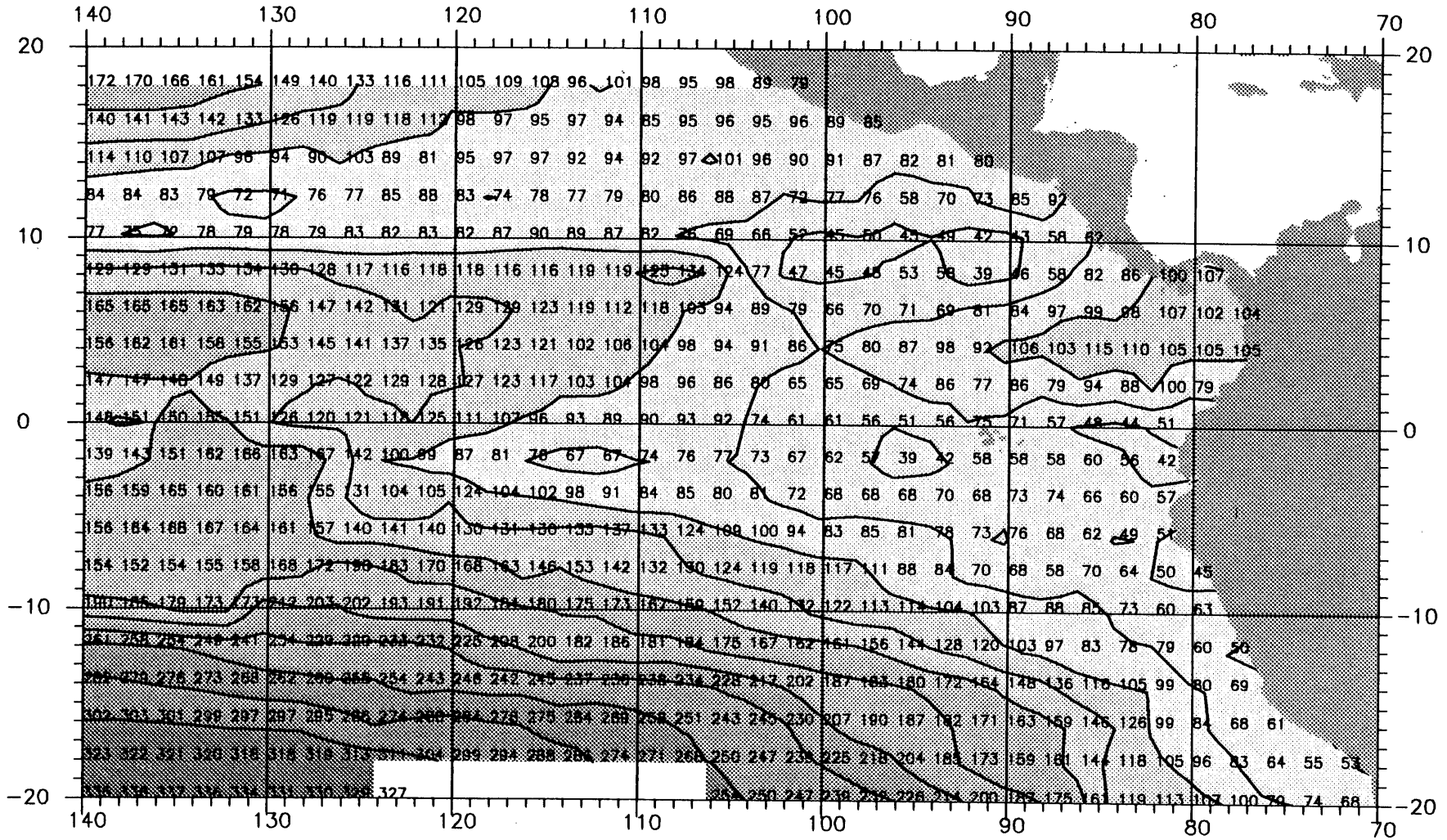

FALL

MAP 11b

RMS DEVIATION (σ_k), METERS

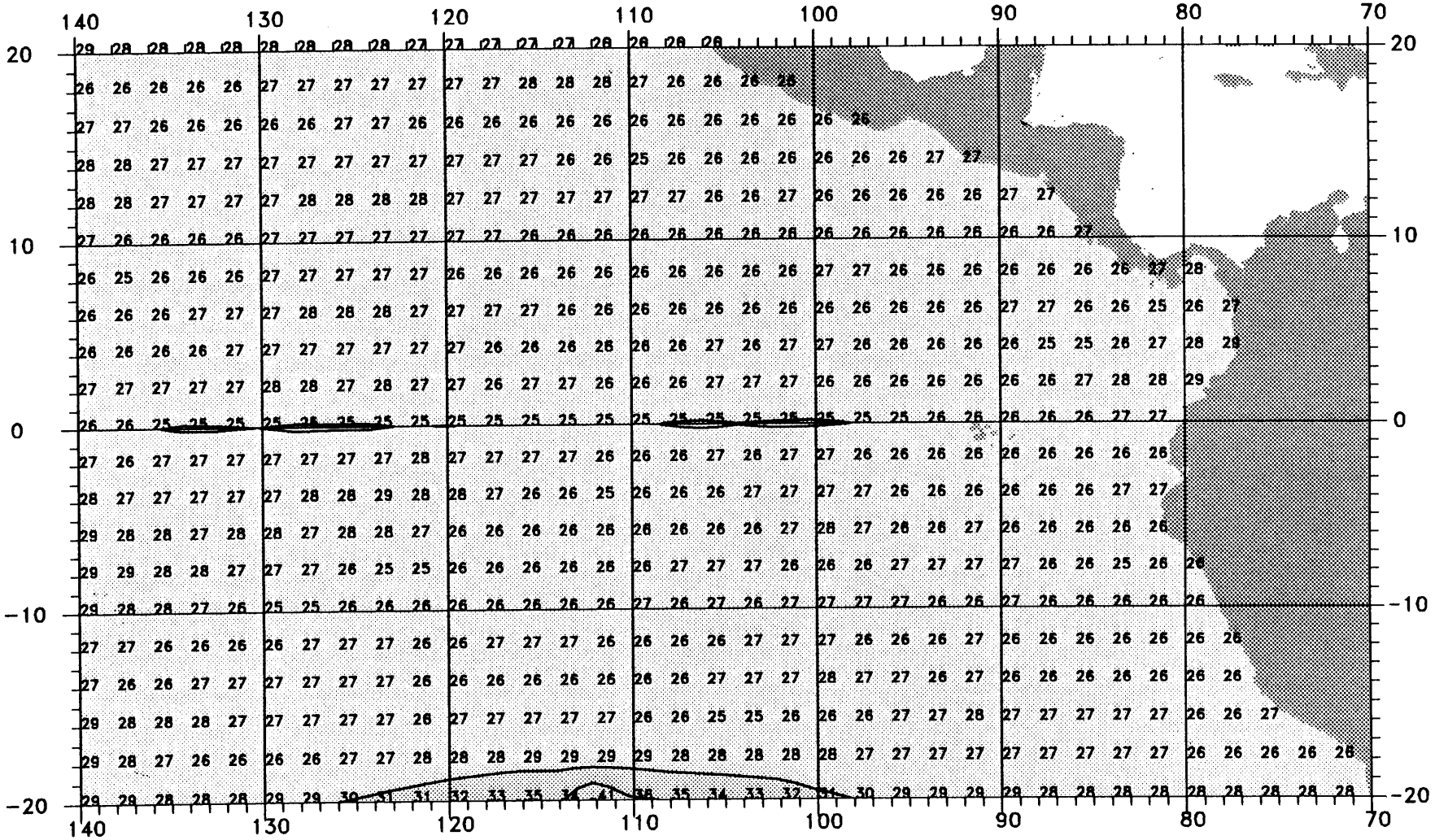

FALL, 10° C

MAP 12a

10° ISOTHERM DEPTH, METERS

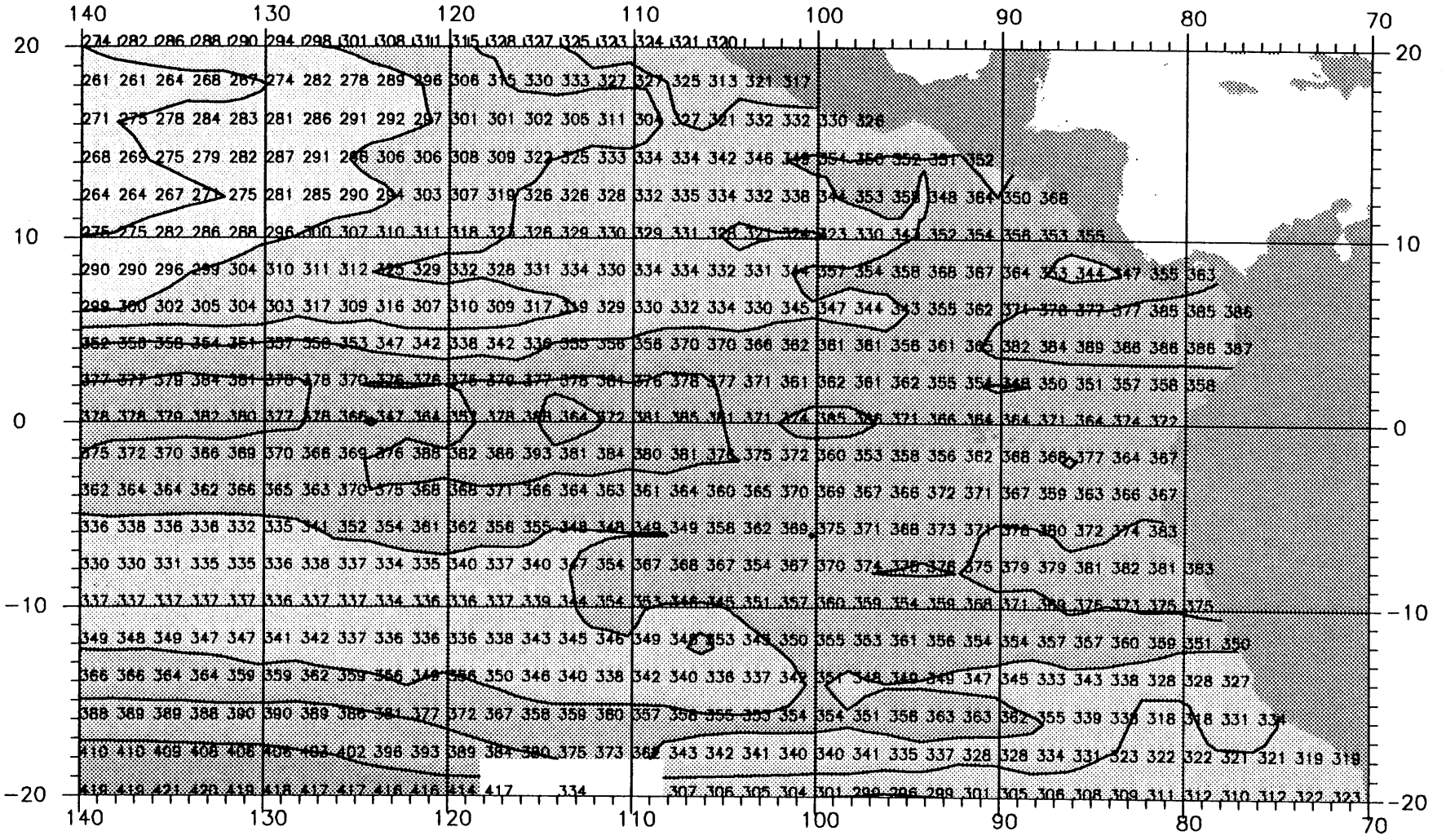

FALL

MAP 12b

* U.S. GOVERNMENT PRINTING OFFICE: 1989 — 673-002/92031